Available at
www.ElsevierComputerScience.com
POWERED BY SCIENCE DIRECT®

Signal Processing 84 (2004) 1177–1199

SIGNAL PROCESSING

www.elsevier.com/locate/sigpro

Singular value decomposition of quaternion matrices: a new tool for vector-sensor signal processing

Nicolas Le Bihan*, Jérôme Mars

Laboratoire des Images et des Signaux, ENSIEG, CNRS UMR 5083, 961 Rue de la Houille Blanche, Domaine Universitaire, B.P. 46, 38402 Saint Martin d'Hères Cedex, France

Received 31 May 2002; received in revised form 30 October 2003

Abstract

We present a new approach for vector-sensor signal modelling and processing, based on the use of quaternion algebra. We introduce the concept of quaternionic signal and give some primary tools to characterize it. We then study the problem of vector-sensor array signals, and introduce a subspace method for wave separation on such arrays. For this purpose, we expose the extension of the Singular Value Decomposition (SVD) algorithm to the field of quaternions. We discuss in more details Singular Value Decomposition for matrices of Quaternions (SVDQ) and linear algebra over quaternions field. The SVDQ allows to calculate the best rank-α approximation of a quaternion matrix and can be used in subspace method for wave separation over vector-sensor array. As the SVDQ takes into account the relationship between components, we show that SVDQ is more efficient than classical SVD in polarized wave separation problem.

Keywords: Vector-sensor array; Quaternion model for vector-sensor signal; Quaternion matrix algebra; Singular Value Decomposition of Quaternion matrix (SVDQ); Subspace method over quaternion field; Polarized wave separation

1. Introduction

Vector-sensor signal processing concerns many areas such as acoustic [25], seismic [1,18], communications [2,16] and electromagnetics [24,25]. A vector-sensor is generally composed of three *components* which record three-dimensional (3D) vibrations propagating through the medium. The *components* of a vector-sensor are, in fact, dipoles in the case of electromagnetic waves and directional geophones in the case of elastic waves. Sensors are positioned close together and record vibrations in three orthogonal directions. A schematic representation of propagation and recording of polarized waves using vector-sensor array is presented in Fig. 1. The use of *multicomponent* sensors allows to recover polarization of the received waves. This physical information is helpful in path recovering and waves identification or classification. Classical approaches in vector-sensor signal processing propose to concatenate the components into a long vector before processing [1,24,25]. In this paper, we propose a different approach to process vector-sensor signals, based on a quaternionic model.

A polarized signal, obtained by recording a polarized wave using a vector-sensor, is a signal which

* Corresponding author. Tel.: +33-4-76-82-64-86; fax: +33-4-76-82-63-84.
E-mail address: nicolas.le-bihan@lis.inpg.fr (N. Le Bihan).

0165-1684/$ - see front matter © 2004 Elsevier B.V. All rights reserved.
doi:10.1016/j.sigpro.2004.04.001

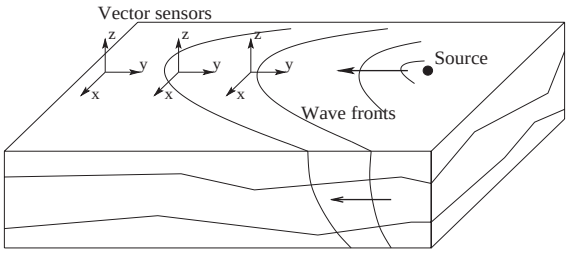

Fig. 1. Schematic representation of a vector-sensor array during a polarized seismic wave acquisition.

samples live in 3D space (in three components vector-sensor case). We define the *quaternionic signal* to be a time series with samples being quaternions. The three components of the signal are placed into the imaginary parts of the quaternion. In this case the possibly non-linear relations between them are kept unchanged. This is not the case when using long-vector approach as this model assume intrinsically that only linear relations exist between components. This motivates the introduction of quaternions to model vector-sensor signals. The quaternionic signal model allows then to develop new tools for vector-sensor signals, based on quaternion algebra.

We concentrate in this paper on the presentation of the extension of a classical and very useful tool in numerical signal processing: the Singular Value Decomposition (SVD). We present the extension of SVD to the quaternion field and we propose a new simple subspace method for vector-sensor signal processing. This new approach (that takes into account relationship between components) is applied on some simulated data.

The paper is organized as follows. In Section 2, we give a brief recall on quaternions and some of their properties. In Section 3, a review of some quaternion linear matrix algebra theorems is presented, as well as a presentation of the isomorphism between quaternion and complex fields. Using this isomorphism, quaternion matrix operations can be computed by means of classical complex matrix computation algorithms. Particular attention is paid to the extension of the SVD to matrices with quaternions entries, called SVDQ. In Section 4, using definition of right Hilbert space from Section 1, we can study the quaternion one-dimensional (1D) signal by means of quaternion vectors, and the bidimensional (2D) signals by means of quaternion matrices. We propose a new model for vector-sensor array signals. This model allows us to manipulate polarized signals and to include polarization property directly in the processing. We also introduce the mixture model for the polarized wave separation technique presented next. Section 5 is devoted to introduction of a new subspace method for wave separation on vector-sensor arrays based on SVDQ. Its efficiency is then evaluated on synthetic polarized dataset in Section 6. Conclusions are given in Section 7.

2. Quaternions

Quaternions are an extension of complex numbers from the 2D plane to the 3D space (as well as 4D space) and form one of the four existing division algebra (real $\mathbb{R}$, complex $\mathbb{C}$, quaternions $\mathbb{H}$ and octonions $\mathbb{O}$). Firstly discovered by Sir Hamilton [12] in 1843, they can be regarded as a special case of *hypercomplex numbers* systems [17]. Quaternion algebra is also the even Clifford algebra Cl_3^+ [21].

Quaternions are mostly used in computer vision because of their ability to represent rotations in 3D and 4D spaces. In fact, a quaternion can represent any rotation of the rotation group SO(3). Also, two quaternions can represent any rotation from the group of rotations SO(4) [21]. Real and complex numbers are special cases of quaternions (i.e. $\mathbb{R} \subset \mathbb{C} \subset \mathbb{H}$).

We now give the definition of quaternions and introduce different notations for them. Then we briefly introduce some basic properties. Interested reader may find some more complete material in [5,10,12,13,17,21].

2.1. Definition

A quaternion q is an element of the 4D normed algebra over the real number with basis $\{1, \mathtt{i}, \mathtt{j}, \mathtt{k}\}$. So, q has a real part and three imaginary parts:

$$q = a + b\mathtt{i} + c\mathtt{j} + d\mathtt{k}, \tag{1}$$

where $a, b, c, d \in \mathbb{R}$, and $\mathtt{i}, \mathtt{j}, \mathtt{k}$ are *imaginary units*. a is called the real part and $q - a$ the *vector* part.

The multiplication rules between the three imaginary numbers are:

$$\mathtt{i}^2 = \mathtt{j}^2 = \mathtt{k}^2 = \mathtt{ijk} = -1,$$

$$\mathtt{ij} = -\mathtt{ji} = \mathtt{k},$$

$$\mathtt{ki} = -\mathtt{ik} = \mathtt{j},$$

$$\mathtt{jk} = -\mathtt{kj} = \mathtt{i}. \tag{2}$$

Note that the multiplication of quaternions is not commutative, and this is due to the relations between the three imaginary parts.[1] Several notations exist for quaternions [5,10,12,13,28]. A quaternion q can uniquely be expressed as

$$q = \alpha + \beta\mathtt{j}, \tag{3}$$

where $\alpha = a + b\mathtt{i}$ and $\beta = c + d\mathtt{i} \in \mathbb{C}$. This is currently known as the Cayley–Dickson notation. α can be seen as the projection of q on the complex plane [15]. We will later use the Cayley–Dickson notation for quaternion matrix processing.

It is well known that the Euler formula also generalizes to quaternion [13]. This allows to interpret quaternions in terms of modulus and phase. Any quaternion $q = a + b\mathtt{i} + c\mathtt{j} + d\mathtt{k}$ can thus be written as

$$q = \rho e^{\xi\theta} \quad \text{with} \quad \begin{cases} \rho = \sqrt{a^2 + b^2 + c^2 + d^2}, \\ \xi = \dfrac{b\mathtt{i} + c\mathtt{j} + d\mathtt{k}}{\sqrt{b^2 + c^2 + d^2}}, \\ \theta = \arctan\left(\dfrac{\sqrt{b^2 + c^2 + d^2}}{a}\right). \end{cases} \tag{4}$$

In this *polar* formulation, ρ is the modulus of q, ξ is a pure unitary quaternion (see Section 2.2 for definition) sometimes called *eigenaxis* [28] and θ is the angle (or *eigenangle* [28]) between the real part and the 3D imaginary (or vector) part. This can be rewritten in a trigonometric version as

$$\begin{aligned} \rho e^{\xi\theta} &= \rho(\cos\theta + \xi\sin\theta) \\ &= \rho(\cos\theta + \sin\theta\cos\phi\sin\psi\mathtt{i} \\ &\quad + \sin\theta\sin\phi\sin\psi\mathtt{j} + \sin\theta\mathtt{k}), \end{aligned} \tag{5}$$

where ϕ and ψ are respectively the azimuth and elevation angles that define the position of ξ in the 3D space. The *polar* notation will be used in the quaternion model for vector signals in Section 4.

2.2. Properties

We now give some properties of quaternions. Interested reader will find an extensive list of quaternions properties in [12,13,17,37]. We focus here on the properties that we need in our work.

The conjugate of a quaternion, $\bar{q}$, is defined as

$$\bar{q} = a - b\mathtt{i} - c\mathtt{j} - d\mathtt{k}. \tag{6}$$

A *pure* quaternion is a quaternion with a null real part ($a = 0$). Quaternions with non-null real parts are sometimes called *full* quaternions.

The norm of a quaternion is

$$|q| = \sqrt{q\bar{q}} = \sqrt{\bar{q}q} = \sqrt{a^2 + b^2 + c^2 + d^2}. \tag{7}$$

q is called a *unit* quaternion if its norm is 1. The inverse of a quaternion is

$$q^{-1} = \frac{\bar{q}}{|q|^2}. \tag{8}$$

Multiplication of quaternions is not commutative. Given two quaternions q_1 and q_2, we have

$$q_1 q_2 \neq q_2 q_1. \tag{9}$$

This property involves the possible definition of two kinds of vector spaces over $\mathbb{H}$. In order to study signals with values in $\mathbb{H}$, we now give some details on the definition of Hilbert spaces over the quaternion field. This definition is necessary for validation of the model that we propose for vector signals in Section 4.

2.3. Quaternion Hilbert space

Here we will consider right vector spaces over $\mathbb{H}$. As said before, $\mathbb{H}$ is a division algebra, and $\mathbb{H}^N$ can be seen as a vector space of dimension N over $\mathbb{H}$. In such a vector space, matrices operate on the opposite side of $\mathbb{H}^N$ compared to scalars. In order to recover classical matrix calculus rules, we choose the convention that matrices operate on the left side, and so scalars operate on the right side. This is why we will use *right* vector spaces here.

[1] Some commutative versions of quaternions, named bicomplex numbers, have been introduced (see [5,10] for details), which have found some applications in digital signal processing [31] and source separation [36].

Definition 1. A vector space of dimension N, namely $\mathbb{H}^N$, over the field of quaternions $\mathbb{H}$ is a *right vector space* if:

$$\forall v \in \mathbb{H}^N \quad \text{and} \quad \forall \zeta, \mu \in \mathbb{H}\text{: } (v\zeta)\mu = v(\zeta\mu). \tag{10}$$

As $\mathbb{H}$ is not commutative, Eq. (10) is not equivalent to the property that holds in the case of left vector spaces over $\mathbb{H}$: $\mu(\lambda v)=(\mu\lambda)v$. In our case (right vector space), the order of factors in matrix multiplication must be carefully kept.

We now introduce some basic definitions needed for quaternionic numerical signal processing over a quaternion Hilbert space.

2.3.1. Quaternion vector

Classically, in numerical signal processing, signals are represented in a Hilbert space. Similarly, for the case of quaternionic signals, we can work on a quaternion Hilbert space. This quaternion Hilbert space is a right vector space. In this Hilbert space, a quaternionic discretized signal of N samples is a vector whose elements are quaternions: $\mathbf{x} = [x_1\ x_2\ \dots\ x_N]^{\mathrm{T}} \in \mathbb{H}^N$, and $x_i \in \mathbb{H}$.

Over this vector space, a scalar product can be defined as

$$\langle \mathbf{x}, \mathbf{y} \rangle = \mathbf{x}^{\triangleleft}\mathbf{y} = \sum_{\alpha=1}^{N} \bar{x}_\alpha y_\alpha, \tag{11}$$

where $\triangleleft$ denotes the quaternion transposition-conjugate operator. Due to the fact that for quaternions we have $\overline{\overline{q_1}q_2} = \overline{q_2}q_1$ (because $\overline{q_1}\overline{q_2} = \overline{q_2}\,\overline{q_1}$ and $\bar{\bar{q}} = q$), the scalar product has the following property:

$$\langle \mathbf{x}, \mathbf{y} \rangle = \overline{\langle \mathbf{y}, \mathbf{x} \rangle}. \tag{12}$$

Two quaternion vectors $\mathbf{x} \in \mathbb{H}^N$ and $\mathbf{y} \in \mathbb{H}^N$ are said orthogonal if $\langle \mathbf{x}, \mathbf{y} \rangle = 0$.

The definition of the *norm* for quaternion vectors is

$$\|\mathbf{x}\| = \sqrt{\langle \mathbf{x}, \mathbf{x} \rangle}. \tag{13}$$

A metric can also be defined in order to measure the distance between two quaternion vectors $\mathbf{x}$ and $\mathbf{y}$:

$$d(\mathbf{x}, \mathbf{y}) = \|\mathbf{x} - \mathbf{y}\| = [(\mathbf{x} - \mathbf{y})^{\triangleleft}(\mathbf{x} - \mathbf{y})]^{1/2}. \tag{14}$$

These definitions are nothing more than the extension to the quaternion case of the classical definitions frequently used in signal processing. We also give here the definition of the outer product of two quaternion vectors.

Given $\mathbf{x} \in \mathbb{H}^N$ and $\mathbf{y} \in \mathbb{H}^M$, their outer product is given by

$$\mathbf{A} = [a_{\alpha\beta}]_{\alpha,\beta} = \mathbf{x} \circ \mathbf{y} = [x_\alpha y_\beta]_{\alpha,\beta}, \tag{15}$$

where $\mathbf{A} \in \mathbb{H}^{N\times M}$ is a rank-1 quaternion matrix. The outer product of $\mathbf{x}$ and $\bar{\mathbf{x}}$ (i.e. $\mathbf{x} \circ \bar{\mathbf{x}}$ or the alternative notation $\mathbf{x}\mathbf{x}^{\triangleleft}$) is a hermitian rank-1 matrix. Rank-1 matrices will be encountered when considering the SVD of quaternion matrices.

2.3.2. Quaternion matrix

A given set of N signals from $\mathbb{H}^M$ (noted $\mathbf{x}_p$ with $1 \leqslant p \leqslant N$) can be arranged in a matrix $\mathbf{X}$ such as

$$\mathbf{X} = \begin{bmatrix} \mathbf{x}_1^{\mathrm{T}} \\ \mathbf{x}_2^{\mathrm{T}} \\ \vdots \\ \mathbf{x}_N^{\mathrm{T}} \end{bmatrix}. \tag{16}$$

This matrix is quaternion valued and defines a vector space $\mathbf{X} \in \mathbb{H}^{N\times M}$. The study of quaternion matrices will be made in Section 3. Such a matrix will be used to represent a set of discretized signals recorded on a vector-sensor array (see Section 4).

2.4. Linear subspaces over quaternion vector spaces

We give here the definitions of basis and subspaces over a quaternion vector space. Recall that we consider here a right vector space as defined in Section 2.3.

Definition 2. Consider a set of vectors, not necessarily linearly independent, $(\mathbf{e}_1, \mathbf{e}_2, \dots, \mathbf{e}_p)$, $\mathbf{e}_\alpha \in \mathbb{H}^N$. The *right span* $\mathscr{S}^r$ of these vectors is the set of all vectors $\mathbf{e} \in \mathbb{H}^N$ that may be generated from linear combination of the set:

$$\mathscr{S}^r(\mathbf{e}_1, \mathbf{e}_2, \dots, \mathbf{e}_p) = \left\{ \mathbf{e}\text{: } \mathbf{e} = \sum_{\alpha=1}^{p} \mathbf{e}_\alpha a_\alpha \right\}, \tag{17}$$

where $a_\alpha \in \mathbb{H}$.

The span $\mathscr{S}^r$ is itself a subspace of $\mathbb{H}^N$. We now introduce the definition of *right* linearly independence for a set of quaternion vectors.

Definition 3. A set of quaternion valued vectors $(\mathbf{e}_1, \mathbf{e}_2, \ldots, \mathbf{e}_p)$ is said to be *right linearly independent* if: $\mathbf{e}_1 c_1 + \mathbf{e}_2 c_2 + \cdots + \mathbf{e}_p c_p = 0$ holds only when $c_1 = c_2 = c_3 = \cdots = c_p = 0$, with $c_\alpha \in \mathbb{H}$.

As in complex and real cases, the concept of a basis over a quaternion vector space can be stated:

Definition 4. If, in the set $(\mathbf{e}_1, \mathbf{e}_2, \ldots, \mathbf{e}_p)$, right linearly dependent vectors are removed and all of the right linearly independent ones are retained, the new set $(\mathbf{e}_{(1)}, \mathbf{e}_{(2)}, \ldots, \mathbf{e}_{(p)})$ is a *right* basis.

We can now introduce the direct subspaces concept:

Definition 5. The right linearly independent set of vectors $(\mathbf{e}_{(1)}, \mathbf{e}_{(2)}, \ldots, \mathbf{e}_{(p)})$ can be divided in m disjoint sets of vectors. Each disjoint set spans its respective subspace $\mathscr{S}_q^r$. Therefore, $\mathscr{S}^r$ can be written as a direct sum of disjoint right linearly independent subspaces:

$$\mathscr{S}^r = \mathscr{S}_1^r \oplus \mathscr{S}_2^r \oplus \cdots \oplus \mathscr{S}_m^r. \tag{18}$$

In the case where the basis is orthogonalized (via a QR process for example), the set $\mathscr{S}^r$ can be expressed as a direct sum of mutually orthogonal subspaces.

Definition 6. The set of vectors can be orthogonalized and the orthogonal set of vectors is noted $(\mathbf{u}_{(1)}, \mathbf{u}_{(2)}, \ldots, \mathbf{u}_{(p)})$ with $\langle \mathbf{u}_{(\alpha)}, \mathbf{u}_{(\beta)} \rangle = 0$ for all $\alpha \neq \beta$. Then $\mathscr{S}^r$ forms a linearly independent orthogonal basis. So the set $\mathscr{S}^r$ can be written as a direct sum of m linear independent and orthogonal subspaces:

$$\mathscr{S}^r = \mathscr{U}_1^r \oplus \mathscr{U}_2^r \oplus \cdots \oplus \mathscr{U}_m^r, \tag{19}$$

where

$$\mathscr{U}_\omega^r = \left\{ \mathbf{e}\colon \mathbf{e} = \sum_{i_\omega \in I_\omega} \mathbf{u}_{i_\omega} b_{i_\omega} \right\} \tag{20}$$

with I_ω the ωth disjoint subset of $\{1, 2, \ldots\}$ and $b_{i_\omega} \in \mathbb{H}$ the coefficients of the vectors in the ωth subset. [2]

Existence of a set of orthogonal quaternion vectors was also postulated in Lemma 5.2 in [37].

[2] In the general case, coefficients b_{i_ω} take values in $\mathbb{H}$. However, as $\mathbb{R} \subset \mathbb{C} \subset \mathbb{H}$, linear combinations of quaternionic vectors with real or complex coefficients can be encountered and are just special cases.

The decomposition in direct orthogonal subspaces will be exploited in the polarized wave separation technique presented in Section 5.

Now, in order to develop some quaternionic signal processing tools, we introduce some elements of quaternion matrix algebra which are the basics needed for vector signal processing.

3. Quaternion matrix algebra

The study of quaternion matrices has been an active field of research for several years, with starting point in 1936 [35], and is still in development. Important research works on this subject were carried out by Zhang [37], Huang and So [15], Thompson [32], among others. In this section, we give some elements of quaternion matrix algebra. After introducing the complex notation for vectors and quaternion matrices, we present the extension of classical matrix algebra concepts to the quaternion field. An extensive summary of the basic properties of quaternion matrices can be found in [3,20,37]. We then give the definition of the SVD of a Quaternion matrix (SVDQ) and propose an algorithm for its computation. We also demonstrate that, as in real and complex case, the SVDQ allows to define the best rank-α truncation of a quaternion matrix.

3.1. Complex representation of a quaternion vector

Definition 7. Given a quaternion vector $\mathbf{x} \in \mathbb{H}^N$ expressed using the Cayley–Dickson notation such as: $\mathbf{x} = \mathbf{x}_1 + \mathbf{x}_2 \mathbf{j}$, with $\mathbf{x}_1$ and $\mathbf{x}_2 \in \mathbb{C}^N$. We can then define a bijection $f : \mathbb{H}^N \to \mathbb{C}^{2N}$ such as

$$f(\mathbf{x}) = \begin{bmatrix} \mathbf{x}_1 \\ -\mathbf{x}_2^* \end{bmatrix}, \tag{21}$$

where $*$ is the complex conjugate operator.

Linear properties are invariant under bijection f. We will see the usefulness of this notation in computing the left and right singular vectors of a quaternion matrix (Section 3.4.1.).

3.2. Complex representation of a quaternion matrix

Definition 8. Given a quaternion matrix $\mathbf{A} \in \mathbb{H}^{N \times M}$, its expression using the Cayley–Dickson notation is

$\mathbf{A} = \mathbf{A}_1 + \mathbf{A}_2\mathrm{j}$, where $\mathbf{A}_1$ and $\mathbf{A}_2$ are complex matrices (i.e. $\in \mathbb{C}^{N\times M}$). One can then define the complex adjoint matrix [37], denoted by $\chi_A \in \mathbb{C}^{2N\times 2M}$, corresponding to the quaternion matrix $\mathbf{A}$, as follows:

$$\chi_A = \begin{pmatrix} \mathbf{A}_1 & \mathbf{A}_2 \\ -\mathbf{A}_2^* & \mathbf{A}_1^* \end{pmatrix}. \tag{22}$$

Some properties of χ_A are given in [20,35,37]. We give here a summary of these properties for given matrices $\mathbf{A}$ and $\mathbf{B} \in \mathbb{H}^{N\times M}$ and their complex adjoint χ_A and $\chi_B \in \mathbb{C}^{2N\times 2M}$:

- χ_A is normal, hermitian or unitary if and only if $\mathbf{A}$ is normal, hermitian or unitary,
- $\chi_{AB} = \chi_A\chi_B$,
- $\chi_{A+B} = \chi_A + \chi_B$,
- $\chi_{A^{-1}} = (\chi_A)^{-1}$ if $\mathbf{A}^{-1}$ exists
- $\chi_{A^\triangleleft} = (\chi_A)^\dagger$,

where † denotes the complex conjugate-transposition operator. This complex notation for quaternion matrices can be used to compute quaternion matrix decomposition using complex decomposition algorithm.

We now focus on some classical matrix properties in the quaternion case.

3.3. Properties of quaternion matrices

We do not intend to list the whole set of properties of matrices of quaternions, but will give those which are useful for our discussion.

3.3.1. Basic operations

Some well-known equalities for complex and real matrices stand for matrices of quaternions, whereas some others are no more valid. Here is a short list of relations that stand for quaternion matrices $\mathbf{A} \in \mathbb{H}^{N\times M}$ and $\mathbf{B} \in \mathbb{H}^{M\times P}$:

- $(\mathbf{AB})^\triangleleft = \mathbf{B}^\triangleleft\mathbf{A}^\triangleleft$,
- $\overline{\mathbf{AB}} \neq \overline{\mathbf{A}}\,\overline{\mathbf{B}}$ in general,
- $(\mathbf{A}^\triangleleft)^{-1} = (\mathbf{A}^{-1})^\triangleleft$,
- $(\overline{\mathbf{A}})^{-1} \neq \overline{\mathbf{A}^{-1}}$ in general.

See [37] for a more complete list. The most common way to study quaternion matrices is to use their *complex adjoint* (complex representation of a quaternion matrix) introduced in [20]. We now give some general definitions for matrices over $\mathbb{H}$.

3.3.2. Rank of a quaternion matrix

Definition 9. As in complex and real matrix case, the rank of a matrix of quaternions $\mathbf{A}$ is the minimum number of quaternion matrices of rank-1 that yield $\mathbf{A}$ by a linear combination.

Property 1. The rank of a quaternion matrix $\mathbf{A}$ is r if and only if the rank of its complex adjoint χ_A is $2r$.

This property was first stated by Wolf [35]. In addition to this definition, we indicate that the rank of $\mathbf{A}$ is r if $\mathbf{A}$ has r non-zero singular values.

3.4. Singular value decomposition of a quaternion matrix (SVDQ)

We study the definition and computation of the SVD for matrices of Quaternions (SVDQ). Regarding the wide use of SVD and its extensions in signal processing [8,9,23,30,34], we can envisage huge potentiality for SVDQ with applications in domains connected to signal and image processing, especially for vector signals and vector images cases. Here we propose to use SVDQ for vector-sensor array processing. The first statement of this decomposition can be found, to our knowledge, in [37].

Proposition 10. *For any matrix* $\mathbf{A} \in \mathbb{H}^{N\times M}$, *of rank* r, *there exist two quaternion unitary matrices*[3] $\mathbf{U}$ *and* $\mathbf{V}$ *such that*

$$\mathbf{A} = \mathbf{U}\begin{pmatrix} \mathbf{\Sigma}_r & 0 \\ 0 & 0 \end{pmatrix}\mathbf{V}^\triangleleft, \tag{23}$$

where $\mathbf{\Sigma_r}$ *is a real diagonal matrix and has r non-null entries on its diagonal* (*i.e. singular values of* $\mathbf{A}$). $\mathbf{U} \in \mathbb{H}^{N\times N}$ *and* $\mathbf{V} \in \mathbb{H}^{M\times M}$ *contain respectively the left and right quaternion singular vectors of* $\mathbf{S}$.

Proof. Demonstration of existence of the SVDQ is given in [37]. It is based on the proof of existence of the polar decomposition for any quaternion matrix. As

[3] A quaternion unitary matrix $\mathbf{W} \in \mathbb{H}^{N\times N}$ has the following property: $\mathbf{W}\mathbf{W}^\triangleleft = \mathbf{W}^\triangleleft\mathbf{W} = \mathbf{I}_N$, with $\mathbf{I}_N \in \mathbb{R}^{N\times N}$ the identity matrix.

polar decomposition and SVD are equivalent (even for quaternion matrices), existence of the polar decomposition induces existence of the SVDQ (see [37] for details). □

The SVDQ can also be written as follows:

$$\mathbf{A} = \sum_{n=1}^{r} \mathbf{u}_n \mathbf{v}_n^{\triangleleft} \sigma_n, \tag{24}$$

where $\mathbf{u}_n$ are the left singular vectors (columns of $\mathbf{U}$) and $\mathbf{v}_n$ the right singular vectors (columns of $\mathbf{V}$). σ_r are the real singular values. This expression shows that the SVDQ, as does the SVD in real and complex case, decomposes the matrix into a sum of r rank-1 quaternion matrices. The SVDQ is hence said to be rank revealing: the number of non-null singular values equals the rank of the matrix.

We now propose a method for the computation of the SVDQ.

3.4.1. Computation of the SVDQ

We propose to compute the SVDQ using the isomorphism between $\mathbb{H}^{N\times M}$ and $\mathbb{C}^{2N\times 2M}$. Notice that quaternion algorithms have, up to now, only been proposed for QR decomposition [6], but no quaternionic algorithm has been proposed for computing the SVDQ.

The singular elements of a quaternion matrix $\mathbf{A}$ can be obtained from the SVD of its *complex adjoint* matrix χ_A. Firstly, recall that χ_A admits a (complex) SVD:

$$\chi_A = \mathbf{U}^{\chi_A} \begin{pmatrix} \mathbf{\Sigma}_{2r} & 0 \\ 0 & 0 \end{pmatrix} (\mathbf{V}^{\chi_A})^{\dagger} = \sum_{n'=1}^{2r} \sigma_{n'} \mathbf{u}_{n'}^{\chi_A} \mathbf{v}_{n'}^{\chi_A \dagger}, \tag{25}$$

where the columns of $\mathbf{U}^{\chi_A}$ and $\mathbf{V}^{\chi_A}$ are elements of $\mathbb{C}^{2N}$ and $\mathbb{C}^{2M}$ respectively and given by

$$\mathbf{u}_{n'}^{\chi_A} = \begin{bmatrix} \dot{\mathbf{u}}_{n'}^{\chi_A} \\ -(\ddot{\mathbf{u}}_{n'}^{\chi_A})^* \end{bmatrix} \quad \text{and} \quad \mathbf{v}_{n'}^{\chi_A} = \begin{bmatrix} \dot{\mathbf{v}}_{n'}^{\chi_A} \\ -(\ddot{\mathbf{v}}_{n'}^{\chi_A})^* \end{bmatrix} \tag{26}$$

with $\mathbf{u}_{n'}^{\chi_A} \in \mathbb{C}^{2N}$ (with $\dot{\mathbf{u}}_{n'}^{\chi_A} \in \mathbb{C}^{N}$ and $\ddot{\mathbf{u}}_{n'}^{\chi_A} \in \mathbb{C}^{N}$) and $\mathbf{v}_{n'}^{\chi_A} \in \mathbb{C}^{2M}$ (with $\dot{\mathbf{v}}_{n'}^{\chi_A} \in \mathbb{C}^{M}$ and $\ddot{\mathbf{v}}_{n'}^{\chi_A} \in \mathbb{C}^{M}$). The special structure of χ_A (see Eq. (22)) induces the structures in $\mathbf{u}_{n'}^{\chi_A}$ and $\mathbf{v}_{n'}^{\chi_A}$ which represent quaternion vectors in their complex notations (see Eq. (21)). This structure in singular vectors of χ_A is always found when considering *complex adjoint matrices*.[4]

Considering the diagonal matrix $\mathbf{\Sigma}_{2r}$, it has the special structure:

$$\mathbf{\Sigma}_{2r} = \operatorname{diag}(\sigma_1; \sigma_1; \sigma_2; \sigma_2; \ldots; \sigma_r; \sigma_r). \tag{27}$$

This structure in the diagonal entries comes from the fact that the singular values of χ_A are the square roots of the eigenvalues of $\chi_A(\chi_A)^{\dagger}$ and $(\chi_A)^{\dagger}\chi_A$.[5]

Now, for recovering the singular values and vectors of $\mathbf{A} \in \mathbb{H}^{N\times M}$ (i.e. σ_n, $\mathbf{u}_n$ and $\mathbf{v}_n$) from the singular elements of $\chi_A \in \mathbb{C}^{2N\times 2M}$, one must proceed that way:

(1) Compute the SVD of χ_A.
(2) Associate the nth right (resp. left) singular vector of $\mathbf{A}$ with the $n' = (2n-1)$th right (resp. left) singular vector of χ_A, using the following equivalences:

$$\mathbf{u}_n = \dot{\mathbf{u}}_{n'}^{\chi_A} + \ddot{\mathbf{u}}_{n'}^{\chi_A} \mathtt{j},$$

$$\mathbf{v}_n = \dot{\mathbf{v}}_{n'}^{\chi_A} + \ddot{\mathbf{v}}_{n'}^{\chi_A} \mathtt{j}, \tag{28}$$

where $\dot{\mathbf{u}}_{n'}^{\chi_A}$, $\ddot{\mathbf{u}}_{n'}^{\chi_A}$ and $\dot{\mathbf{v}}_{n'}^{\chi_A}$, $\ddot{\mathbf{v}}_{n'}^{\chi_A}$ are given in Eq. (26).
(3) Affect the nth element of the diagonal matrix $\mathbf{\Sigma}_r$ (Eq. (23)), with the $n' = (2n-1)$th diagonal element of the diagonal matrix $\mathbf{\Sigma}_{2r}$ (Eq. (25)).

The computation of the SVDQ for a $N \times M$ quaternion matrix is equivalent to the computation of the SVD of a $2N \times 2M$ complex matrix (its complex adjoint) which can be performed using classical algorithms of SVD over $\mathbb{C}^{2N\times 2M}$ [11].

3.5. Best rank-α approximation of a quaternion matrix

The *Best rank-α approximation* investigates the problem of the approximation of a given matrix, in

[4] This is due to the fact that left and right singular vectors of χ_A are the eigenvectors of $\chi_A(\chi_A)^{\dagger}$ and $(\chi_A)^{\dagger}\chi_A$. Now, $\chi_A(\chi_A)^{\dagger} = \chi_{\mathbf{A}\mathbf{A}^{\triangleleft}}$ and $(\chi_A)^{\dagger}\chi_A = \chi_{\mathbf{A}^{\triangleleft}\mathbf{A}}$, which are *complex adjoint matrices* themselves. It was shown in [22,37] that eigenvectors of any *complex adjoint matrix* have the special structure given in Eq. (21).

[5] Eigenvalues of *complex adjoint matrices* appear by conjugate pairs along the diagonal, and as $\chi_A(\chi_A)^{\dagger}$ is hermitian, its eigenvalues are real and appear by pairs along the diagonal (see [37] for details). So does the singular values of χ_A and this induces the special structure of $\mathbf{\Sigma}_{2r}$.

an optimal least-squares sense, by a matrix of fixed rank-α. In real and complex cases, the solution is obtained by the truncation of the SVD (see [29] for example). We show here that in the quaternion case, the truncation of the SVDQ also gives the best rank-α approximation of a matrix.

Proposition 11. *Consider a matrix* $\mathbf{A} \in \mathbb{H}^{N\times M}$, *with its SVDQ given by Eq.* (24). *Define* $\mathbf{A}_\alpha$, *composed of the* α *first* singular elements (*noted* $\mathscr{A}_n$) *of the SVDQ of* $\mathbf{A}$. $\mathbf{A}_\alpha$ *is the rank-*α *truncation of* $\mathbf{A}$ *and can be written as*

$$\mathbf{A}_\alpha = \sum_{n=1}^{\alpha} \mathscr{A}_n, \tag{29}$$

where a singular element is given by $\mathscr{A}_n = \mathbf{u}_n \mathbf{v}_n^{\lhd} \sigma_n$. *Matrices* $\mathscr{A}_n$ *have ranks equal to* 1, *and so* $\mathbf{A}_\alpha$ *is a rank-*α *matrix. Thus defined,* $\mathbf{A}_\alpha$ *is the* Best rank-α approximation *of* $\mathbf{A}$.

Proof. The square error between the original matrix and the rank-α truncation is

$$\varepsilon^2 = \mathrm{tr}[(\mathbf{A} - \mathbf{A}_\alpha)^{\lhd}(\mathbf{A} - \mathbf{A}_\alpha)], \tag{30}$$

where tr is the trace operator. Using the *complex adjoint* notation for quaternion matrices, we obtain the equivalent equation:

$$\varepsilon_{\mathbb{C}}^2 = \mathrm{tr}[(\chi_A - \chi_{A_{2\alpha}})^{\lhd}(\chi_A - \chi_{A_{2\alpha}})]. \tag{31}$$

This error is called the *Frobenius norm* of $\chi_A - \chi_{A_{2\alpha}}$. Assuming that the truncation of rank 2α of χ_A is

$$\chi_{A_{2\alpha}} = (\mathbf{U}^{\chi_A})\mathbf{\Sigma}_{2\alpha}(\mathbf{V}^{\chi_A})^{\dagger}, \tag{32}$$

where $\mathbf{\Sigma}_{2\alpha} = \mathrm{diag}[\sigma_1;\sigma_1;\sigma_2;\sigma_2;\ldots;\sigma_\alpha;\sigma_\alpha,0,\ldots,0]$, then it can be demonstrated [29] that

$$\varepsilon_{\mathbb{C}}^2 = \sum_{n=2\alpha+1}^{2r} \sigma_n^2. \tag{33}$$

Remember that the singular values of χ_A are the same as those of $\mathbf{A}$. χ_A has twice more singular values due to its construction formula and size. Therefore, if (30) is used, the square error expression will be similar to (33), with twice less values for the index n and so $\varepsilon^2 = \varepsilon_{\mathbb{C}}^2$. □

A property of the error is that it is orthogonal to the approximated matrix $\mathbf{A}_\alpha$. This is true for χ_A as well as for $\mathbf{A}$:

$$(\mathbf{A} - \mathbf{A}_\alpha)\mathbf{A}_\alpha^{\lhd} = 0. \tag{34}$$

This makes the rank-α truncation of the SVDQ of a quaternion matrix the *Best rank-*α *approximation* of the matrix, in the mean square sense [29].

4. Quaternionic model for vector-sensor signals

Signals recorded on a vector-sensor array are often arranged in a long-vector form [1,24,25] before processing, or sometimes, processed component-wise. The use of long-vectors may be restrictive if all possible ways to build this vector are not examined [7,19]. A consequence of processing components separately is that the relations between the signal components are not taken into account. The approach proposed here avoid component-wise and long-vector techniques and aim to process vector signals in a concise way using quaternionic signals.

4.1. Quaternionic signals

In order to process simultaneously the whole data set and to preserve the polarization relations, we propose to encode vector-sensor signals as quaternion valued signals. Such a model allows to extend the concept of modulus and phase to vector-signals having samples evoluting in 3D space. The module is linked with signal magnitude while the 3D phase is directly representative of the 3D Lissajous plot (polarization curve).

4.1.1. Single polarized signal

In the case of a vector-sensor made of three orthogonal components (x, y and z), each one recording a signal of M time samples, we can write the set of three discretized signals ($x(m)$, $y(m)$ and $z(m)$, with $m = 1,\ldots,M$) in a quaternionic single one, $s(m)$ such as

$$s(m) = x(m)\mathtt{i} + y(m)\mathtt{j} + z(m)\mathtt{k}. \tag{35}$$

This model is close to the one given by Sangwine [27] for representing colour images. [6]

[6] In Sangwine's work, the three imaginary parts of a pure quaternion are used to represent the red, blue and green components of a pixel. Notice that in the colour image case, no polarization relations exist between colour channels, but the pixel value lives also in 3D space.

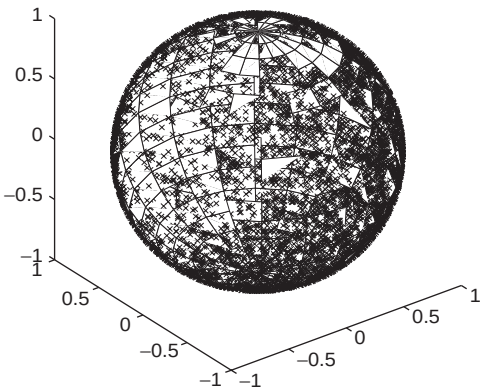

Fig. 2. Three-dimensional plot of the eigenaxis of an unpolarized white Gaussian noise. Each point on the $\mathscr{S}^2$ sphere corresponds to a position of the eigenaxis at a given time.

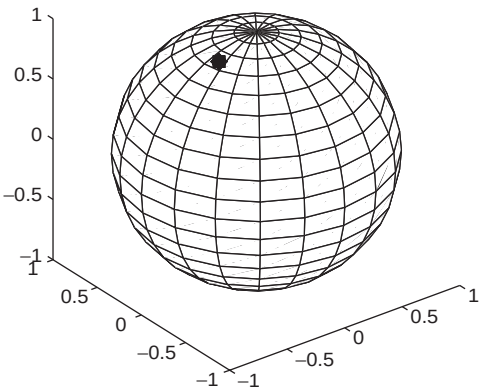

Fig. 3. Three-dimensional plot of the eigenaxis of a linearly polarized Gaussian noise. Each point on the $\mathscr{S}^2$ sphere corresponds to a position of the eigenaxis at a given time.

Here, we consider a vector-sensor array composed of N $(n=1,\ldots,N)$ three components vector-sensors. The quaternionic signal recorded on the sensor at position n, noted $s_n(m)$, can be written using *polar* notation (Eq. (5)):

$$s_n(m)=\rho_n(m)e^{\xi_n(m)\pi/2}=\rho_n(m)e^{\mu_n(m)} \tag{36}$$

with $\xi_n(m)\pi/2=\mu_n(m)$. The angle between real and imaginary part of the quaternionic signal equals $\pi/2$ here as the real part is null (cf. Eq. (5)). Considering the quaternionic signal described in (36), it is possible to understand the signal into its envelope part and its phase term (which is a 3D phase). So, the 3D curve described by $\mu_n(m)$ between $t=1$ and $t=M$ is linked with the polarization of the recorded wave. It is in fact a normalized version of its Lissajous plot. As examples, we present in Figs. 2–4, behaviours of $\mu(m)$ for three different cases: the linearly polarized, the elliptically polarized and the non-polarized case.

In Fig. 2, signals $x(m)$, $y(m)$ and $z(m)$ are three independent Gaussian noises, so no relations exist between them and $\mu(m)$ is distributed over the whole surface of the sphere (i.e. $\mathscr{S}^2$). In Fig. 3, signals $y(m)$ and $z(m)$ are of the form $\alpha x(m)$, with $\alpha\in\mathbb{R}$. There exists a linear relation (polarization is said to be linear) between the three components. So, $\mu(m)$ takes two values on the sphere that can be connected with a line (second value is not visible on the figure as it is masked by the sphere, but as the line passes through the origin, one can easily guess where this point is by point symmetry). In Fig. 4, $y(m)$ and $z(m)$ are of the form α. $\Phi[x(m)]$ where $\alpha\in\mathbb{R}$ and operator $\Phi[.]$ consists in phase shifting the considered signal (explicit expression of $\Phi[.]$ is given in Section 4.1.2). Phase shifts and amplitude ratios between components of the vector signal induces an elliptical behaviour of the eigenangle $\mu(m)$.

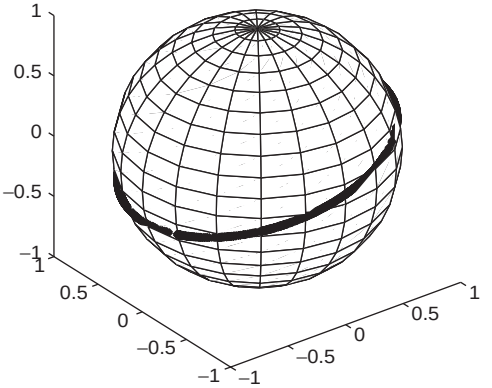

Fig. 4. Three-dimensional plot of the eigenaxis of an elliptically polarized Gaussian noise. Each point on the $\mathscr{S}^2$ sphere corresponds to a position of the eigenaxis at a given time.

This three examples illustrate how $\mu(m)$ render the polarization relations between the components of vector signals. We now investigate the effect of a phase shift on an elliptically polarized vector signal.

4.1.2. Attenuation and phase shift of a polarized signal

During propagation of polarized waves, the medium can affect the waveform by attenuating or phase shifting it (for example when the medium is anisotropic). Attenuation consists in multiplication of the polarized waveform by a real scalar, while phase shift consists in a rotation of its *eigenaxis* in the 3D space (a proof of this correspondence between phase shift and 3D rotation is given in Appendix A). Thus, an attenuated (by a factor α) and shifted (of a quantity ω) polarized signal $s^{\star}(m)$ can be represented as

$$s^{\star}(m) = \alpha\rho(m)\mathrm{e}^{\omega\mu(m)\omega^{-1}}, \tag{37}$$

where $\alpha \in \mathbb{R}$ and $\omega \in \mathbb{H}$, with $|\omega| = 1$. The $\omega\mu(m)\omega^{-1}$ term consists in a rotation of the original *eigenaxis* (see [17] for rotations using quaternions). Notice that the phase shift is no more an angle here (like it is for 1D signals) but a quaternion that represent a rotation in 3D space.

It must be noticed that the most general case of phase shifting for three components sensors would be that propagation introduces three different phase terms on the three components. A more special case is when the three components are phase shifted of the same quantity. This also correspond to a rotation in 3D space of the Lissajous plot. This is what happens in the case of dispersive waves (Section 4.1.4.).

4.1.3. Multisensors polarized signals

Now considering a set of N vector-sensors, the collected vector data set $\mathbf{S}$ can be written as a matrix whose rows are the signals recorded on vector-sensors that constitute the array

$$\mathbf{S} = \begin{bmatrix} s_1(m) \\ s_2(m) \\ \vdots \\ s_N(m) \end{bmatrix}. \tag{38}$$

In this way, the set of signals recorded on the vector-sensor array, $\mathbf{S}$, is a matrix of size $N \times M$ which elements are pure quaternions (i.e., $\mathbf{S} \in \mathbb{H}^{N\times M}$).

4.1.4. Dispersive waves

Dispersive waves are guided waves having different *phase* and *group* velocities. *Group velocity* corresponds to the velocity of the wave packet while *phase velocity* corresponds to the velocity of wave ripples. These concepts are well known in Physics, see for example [4] for details.

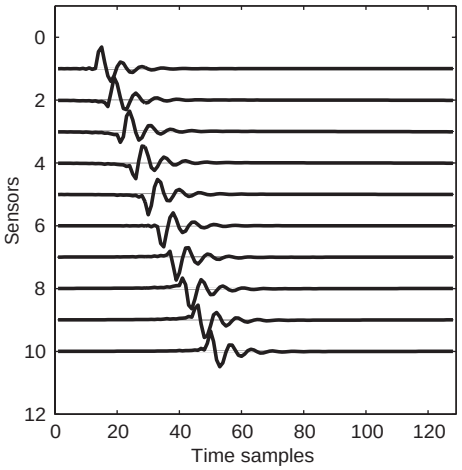

Fig. 5. Dispersive wave collected on single-component sensors. Group velocity (wave packet velocity) and phase velocity (ripples velocity) are different.

Consider now a set of N vector-sensors recording a dispersive wave. As *group* velocity is the velocity of the wave packet, it will correspond to the velocity of the envelope of the quaternionic vector-signal recorded (i.e. of $|s^{\star}(m)| = \rho(m)$). The wave propagation velocity induces a constant time delay τ between signals recorded on two adjacent sensors. So that the delay between the first sensor and the last one of the array is $(N-1)\tau$ (for an array with N sensors). As an example, one component of a dispersive wave is presented in Fig. 5.

The slope of the wave packet on the "sensors vs. time samples" representation can be related to the propagation velocity of the wave. Waves impinging the whole set of sensors at the same time are said to have *infinite velocity* (see Fig. 6). Such configuration happens after velocity correction (see details in Section 4.3).

The difference between *phase* and *group* velocity corresponds to a constant phase shift from one sensor to an other. Such effect also exists when considering sets of scalar sensors [33]. We consider here that for such dispersive waves, the signal recorded on the $(n+1)$th sensor is a phase shifted (of a constant

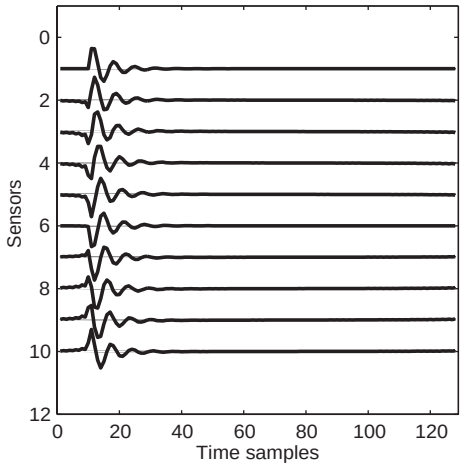

Fig. 6. Dispersive wave collected on single-component sensors, after group velocity correction. The wave packets impinge every sensor at the same time. Phase velocity is not corrected. This wave is said to be with *finite* (*group*) *velocity*.

quantity ω) version of signal recorded at the nth sensor. Assuming, that the signal recorded on the first sensor has an arbitrary phase $\mu(m)$, the signal recorded on the nth sensor can be written as

$$s_n^{\star}(m) = \rho(m)\mathrm{e}^{q^{(n-1)}\mu(m)q^{-(n-1)}}. \tag{39}$$

So phase shift only affects the *eigenaxis* of the quaternionic signal. We will show in Section 5 that this phase shift does not affect the dimension of the subspace necessary for characterisation of the dispersive wave.

4.2. Quaternionic noise

We briefly introduce the concept of *white quaternionic noise* that will be encountered in the mixture model in Section 4.3.

Definition 12. Consider a three-components *centered* noise $b(m)$ recorded on a single vector-sensor. Such a noise is said *quaternionic unpolarized white and Gaussian* if

$$b(m) = b_x(m)\mathtt{i} + b_y(m)\mathtt{j} + b_z(m)\mathtt{k}, \tag{40}$$

where $b_x(m)$, $b_y(m)$ and $b_z(m)$ are Gaussian white noise (with variances γ_x, γ_y and γ_z, and with $\mathbf{E}[\mathbf{b}\mathbf{b}^{\mathrm{T}}] = \mathrm{diag}(\gamma_x, \gamma_y, \gamma_z)$, where $\mathbf{b} = [b_x(m)\ b_y(m)\ b_z(m)]^{\mathrm{T}}$).

There is no relations between components of a such noise (so it is said unpolarized), and considering its polar notation (Eq. (5)), its eigenangle has a behaviour similar to the one given in Fig. 2.

4.3. Mixture model

We now present the mixture model that will be used in the polarized wave separation technique (Section 5).

4.3.1. General model

The received signal on the nth sensor results from the superposition of P (possibly dispersive) polarized waves $g_p(m)$. These waves have propagated through a medium (supposed isotropic) that only affect waves by attenuating, time delaying or phase shifting them. Possibly, additive zero-mean Gaussian white quaternionic noise $b_n(m)$ is recorded:

$$s_n(m) = \sum_{p=1}^{P} h_{np} g_p(m - (n-1)\tau_p) + b_n(m) \tag{41}$$

with $h_{np} \in \mathbb{R}$ the magnitude of wave p at sensor n, $g_p(m) \in \mathbb{H}^N$ the normalized quaternionic (polarized) waveform of wave p. τ_p is the time delay of waveform p between two consecutive sensors. This delay is linked (via the distance between sensors Δm) with the waveform velocity c_p : $\tau_p = \Delta m / c_p$. $b_n(m)$ is supposed spatially white, unpolarized and independent from the source waves. Spatial whiteness induces that two quaternionic noises collected on two different sensors are decorrelated:

$$\langle b_\alpha(m), b_\beta(m) \rangle = \gamma^2 \delta_{\alpha\beta}, \tag{42}$$

where γ^2 is the variance of the centered noise (i.e. squared norm of the quaternion vector corresponding to $b(m)$) and $\delta_{\alpha\beta}$ is the Kronecker delta. [7]

Clearly, the mixture considered here (Eq. (41)) is an instantaneous mixture.

4.3.2. Pre-processing

The pre-processing step consists in applying a group velocity correction to a given wave (here $p=1$), in order that its group velocity becomes *infinite*

[7] $\delta_{\alpha\beta} = \begin{cases} 1 & \text{if } \alpha = \beta, \\ 0 & \text{if } \alpha \neq \beta. \end{cases}$

(i.e. $\tau_1 = 0$, waveforms arriving simultaneously on the whole set of vector-sensors). This pre-processing step can be visualized by the action that leads from Figs. 5 to 6. If pre-processing is operated on g_1, the mixture given in (41) becomes

$$s_n(m)=h_{n1}g_1(m)+\sum_{p=2}^{P}h_{np}g_p(m-(n-1)\tau'_p)+b'_n(m), \tag{43}$$

where τ'_p and $b'_n(m)$ are the modified time delays of other waves and the modified noise (due to delay correction to have $g_1(m)$ with *infinite velocity*).

The quaternion subspace method presented in next section exploits the low rank dimension of a the subspace necessary to represent an infinite velocity wave $g_1(m)$ and thus separate it from the other waves and noise (under orthogonality assumption).

5. Quaternionic subspace method for polarized wave separation

A direct and simple method to process wave separation on a real-valued 2D dataset is to decompose the original vector space defined by the data into two orthogonal subspaces, one called the "signal subspace" and the other one the "noise subspace". This well-known decomposition technique [29] is based on the SVD of the original data set and can be extended to a vector-sensor 2D dataset, using the SVDQ presented above.

5.1. SVDQ and orthogonal subspaces

As stated in Section 2.4, it is possible to decompose a quaternionic vector space into two orthogonal subspaces. Now, considering that a given quaternion matrix $\mathbf{S}\in\mathbb{H}^{N\times M}$ defines such a vector space, its decomposition in two orthogonal subspaces can be directly obtained from its SVDQ. The first subspace is spanned by the singular vectors corresponding to highest singular values and the second one is spanned by the last singular vectors. This can written as

$$\mathbf{S}=[\mathbf{U}_1\,|\,\mathbf{U}_2]\left[\begin{array}{cc|c} \Sigma_1 & 0 & 0 \\ 0 & \Sigma_2 & \\ \hline & 0 & 0 \end{array}\right]\left[\begin{array}{c} \mathbf{V}_1^{\triangleleft} \\ \hline \mathbf{V}_2^{\triangleleft} \end{array}\right]=\mathbf{S}_1+\mathbf{S}_2, \tag{44}$$

where $\mathbf{S}_1$ is the subspace generated by the rank-α truncation of the SVDQ of $\mathbf{S}$ (α highest singular values). Assuming $\mathbf{S}$ has rank r, then $\mathrm{rank}(\mathbf{S})=\mathrm{rank}(\mathbf{S}_1)+\mathrm{rank}(\mathbf{S}_2)$ (i.e. $\mathrm{rank}(\mathbf{S}_1)=\alpha$ and $\mathrm{rank}(\mathbf{S}_2)=r-\alpha$). The use of SVDQ to build the subspaces ensures orthogonality between them in the sense of the inner product defined in (11):

$$\langle\mathbf{u}_p^{(1)},\mathbf{u}_q^{(2)}\rangle=0 \quad\text{and}\quad \langle\mathbf{v}_p^{(1)},\mathbf{v}_q^{(2)}\rangle=0 \tag{45}$$

for any $p=1,\ldots,\alpha$ and $q=\alpha+1,\ldots,r$; where $\mathbf{u}^{(1)}$ and $\mathbf{v}^{(1)}$ (resp. $\mathbf{u}^{(2)}$ and $\mathbf{v}^{(2)}$) are columns of $\mathbf{U}_1$ and $\mathbf{V}_1$ (resp. $\mathbf{U}_2$ and $\mathbf{V}_2$).

We will exploit the orthogonality between subspaces to develop a wave separation technique for vector-sensor 2D array.

5.2. Polarized wave separation

Consider a set of N signals, $s_n(m)$, collected on a vector-sensor array, as introduced in Section 4.1. Thus, following the quaternionic signal model, the data set can be arranged in a quaternion matrix $\mathbf{S}\in\mathbb{H}^{N\times M}$. This quaternionic data set is a mixture of polarized waves and noise. Assuming that a pre-processing step has been performed in order to have one polarized wave that has infinite velocity, $\mathbf{S}$ can be written using the mixture model presented in Eq. (43).

The aim of the technique presented here is to estimate the *infinite velocity* wave and to remove it from the data set. In order to do so, the quaternion matrix $\mathbf{S}$ is decomposed into orthogonal subspaces called *signal subspace* and *noise subspace* like:

$$\mathbf{S}=\mathbf{S}_{\text{signal}}+\mathbf{S}_{\text{noise}}. \tag{46}$$

According to the SVDQ definition (Eq. (24)), it is possible to rewrite the decomposition into subspaces as

$$\mathbf{S}=\sum_{n=1}^{\alpha}\mathbf{u}_n\mathbf{v}_n^{\triangleleft}\sigma_n+\sum_{n=\alpha+1}^{r}\mathbf{u}_n\mathbf{v}_n^{\triangleleft}\sigma_n, \tag{47}$$

where r is the rank of $\mathbf{S}$. As SVDQ is a canonical decomposition of the original quaternion data set, it expresses $\mathbf{S}$ as a sum of r rank-1 matrices. The signal subspace is then constructed with the rank-α truncation of $\mathbf{S}$ and the noise subspace with the remaining part of $\mathbf{S}$ (sum of the $r-\alpha$ other rank-1 matrices).

Determination of α is done by looking at the set of singular values (see for example Fig. 9) and finding a gap in the set. The α highest singular values are then kept to build the *signal subspace*. As independence is stated in the mixture, the orthogonal bases estimated with the SVDQ do not lead to a separation into independent subspaces. As a consequence, the *signal subspace* will contain some noise (in fact the noise can be seen as a quaternionic full rank matrix as it is spatially white, and so some parts of the noise will remain in the rank-α truncation of the original data set).

Practically, the pre-processing ensures that the *infinite velocity* wave $s_1(m)$ is represented by a rank-1 matrix ($\mathbf{S}_{\text{signal}}$, with $\alpha = 1$). Waves with finite velocity are full rank matrices, and thus are considered as noise in the processing. Links between subspaces rank and polarized waves are presented in Appendix B. To summarize, the proposed subspace method lead to an estimate of the *infinite velocity* using a rank-1 truncation of the original matrix $\mathbf{S}$ that is corrupted by the part of the additive noise which is spatially and temporally correlated with the wave.[8] The technique is still valid for small rank of *signal subspace* ($\alpha > 1$) if there remains a significant gap in the set of singular values. The larger is the rank of the *signal subspace*, the more one get some unexpected correlated noise in it.

In the following section, we present some simulation results showing the behaviour of the subspace technique based on SVDQ, as well as comparison with results obtained using a component-wise approach.

6. Simulation results

In the following simulations, the number of sensors is $N = 10$ and the number of time samples is $M = 128$. For each example, quaternionic and component-wise approaches results are presented. The component-wise approach consists in performing (real) subspaces decompositions separately on the three real matrices that contain array signals of the three components.

[8] Recall that correlation is taken in the sense of the quaternionic scalar product.

6.1. Example 1: One elliptically polarized wave added with noise

The three components of the original simulated polarized wave with *infinite velocity* are presented in Fig. 7. In Fig. 8, the mixture consists in the wave and some additive noise. The three components are presented, as three pure imaginary parts of a quaternion matrix (Fig. 8) using the quaternion model.

Singular values of the quaternionic mixture matrix are presented in Fig. 9. Due to the *infinite velocity* polarized wave, one singular value has greater magnitude than the others (see Fig. 9). So the signal subspace will be constructed using a rank-1 truncation of the SVDQ. Result obtained for the signal subspace is presented in Fig. 11.

In order to compare the SVDQ with the component-wise approach, SVD is computed on the three components independently. The three sets of singular values are presented in Fig. 10. It can be seen that one of the singular values is greater in each of the three sets. However, the ratio between the first and the second singular values in the three sets is always lower than the ratio in the SVDQ case. For example, on the j component singular values set, the first singular value is not so different from the others. This is because the wave is buried in noise on this component, and because the magnitude of noise is spread on all singular values with a relatively high level. This does not allow to distinct a singular value among others (that could be attributed to the polarized wave). For this reason, there is no possibility of distinction between signal and noise part when computing this component independently.

The component-wise signal subspace has been constructed using a rank-1 truncation of the SVD for each component. It is presented in Fig. 12.

The correspondence between the original polarized wave (Fig. 7) and the signal subspace obtained by SVDQ (Fig. 11) shows that the technique gives satisfying results. Although noise corrupts the wave front, it is possible to distinguish the coherent wave from the ambient noise (Fig. 11). In particular, on component j of the mixture (Fig. 8), where the wave is buried in the noise, the SVDQ based technique allows to recover the wave. On the opposite, the component-wise approach does not lead to good estimation of the original wave. The result is presented in Fig. 12. One can

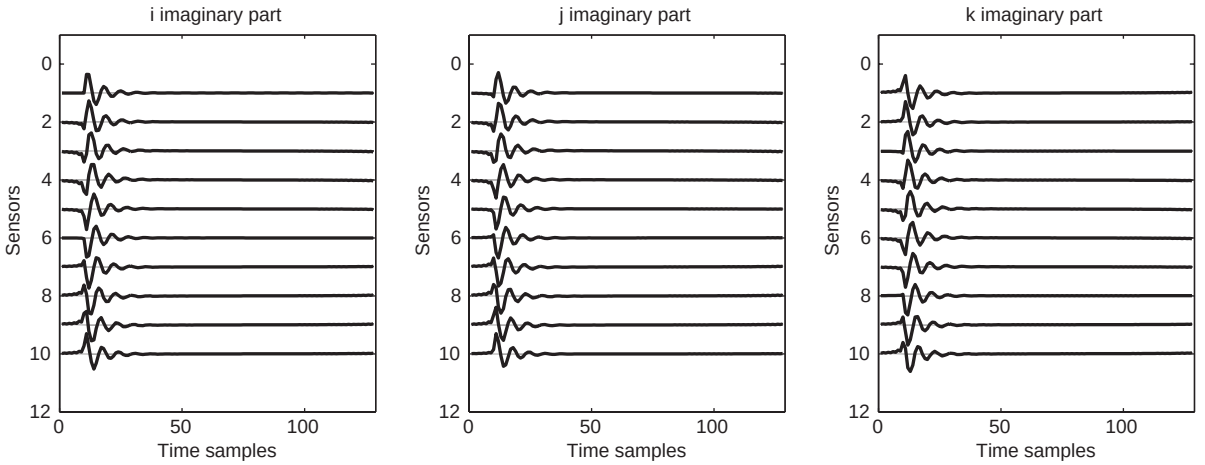

Fig. 7. Original signal with infinite envelope velocity recorded on three components array.

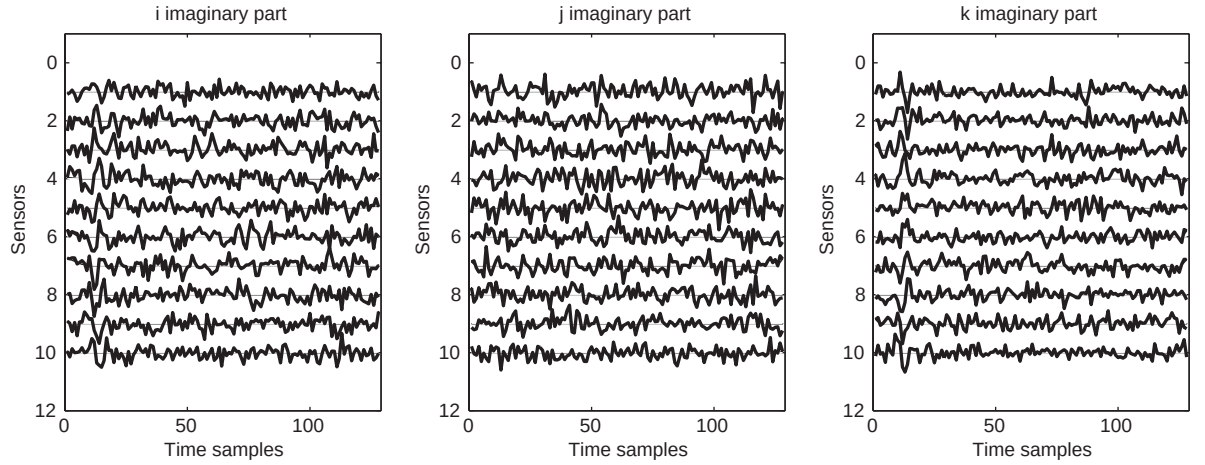

Fig. 8. Mixture 1: one wave and noise.

see that the *signal subspace* obtained in Fig. 12 is corrupted by noise, and the wave is not fully recovered.

By computing each component separately, the component-wise approach does not take advantage of the relations between the components (polarization property) and the wave front is not correctly estimated. This result shows that the quaternion model approach gives better results by taking advantage of the relationship between signal components (Fig. 11).

Also, this example shows that the wave is recovered on the three components, and even on the j component, where its component was not viewable in the mixture (Fig. 8). This indicates that the use of the all components simultaneously in the processing, allows to extract signal components that were lost in noise. Phase shifts and magnitude ratio are recovered for the signal part, which means that an identification of the estimated wave is possible after the processing, using the estimated polarization. This is not possible using the component-wise technique and, in such cases, the SVDQ is required to enhance signal to noise ratio and estimate the polarization of the wave.

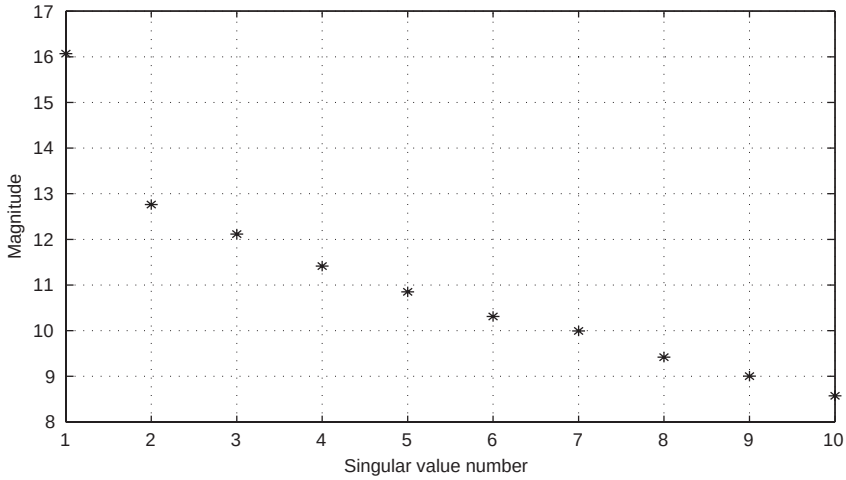

Fig. 9. Mixture 1: singular values obtained by SVDQ.

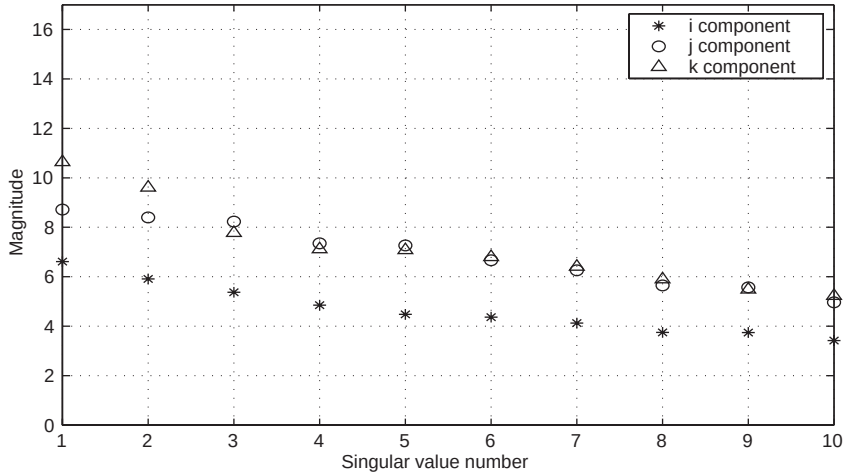

Fig. 10. Mixture 1: singular values obtained by SVD independently on the three components.

6.2. *Example 2: Several polarized waves corrupted by noise*

In this example, it is shown how a dispersive wave with strong magnitude and elliptical polarization can be extracted from the original data. After estimating this wave, the other waves with lowest amplitudes can be recovered. The considered mixture is presented in Fig. 13. It is made of four waves corrupted by noise. One wave has greater amplitude on the three components, and has an infinite velocity (pre-processing step has been performed). This first wave is also a *dispersive wave* (see Section 4.1.4.). Other ones have lower magnitude on different components and are also dispersive waves. All the waves that are in the mixture have different elliptical polarizations.

As in the first example, the SVDQ and the SVD techniques are compared on this data set. In Figs. 14 and 15, we present respectively the set of singular values obtained by SVDQ and the three sets of singular values obtained by component-wise SVD.

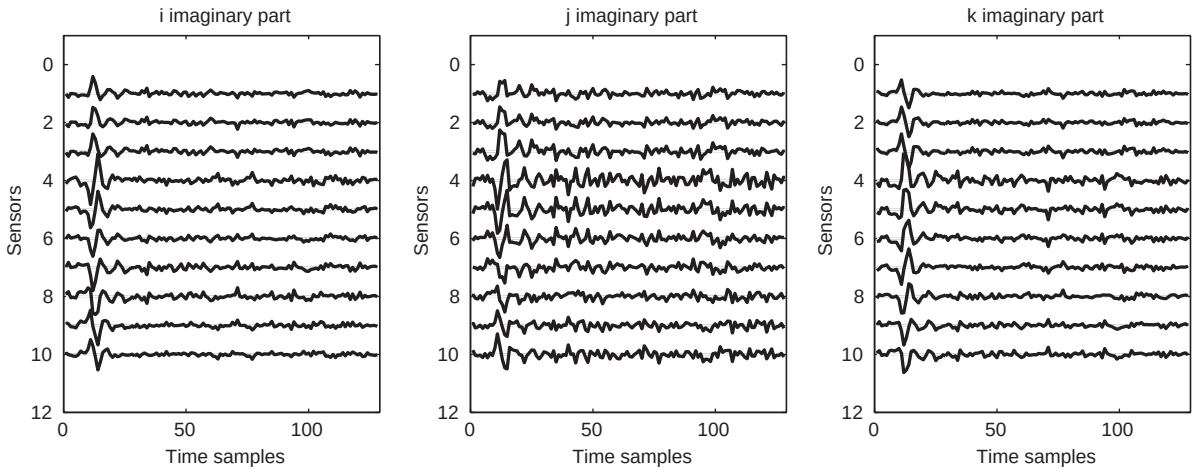

Fig. 11. Mixture 1: signal subspace using SVDQ.

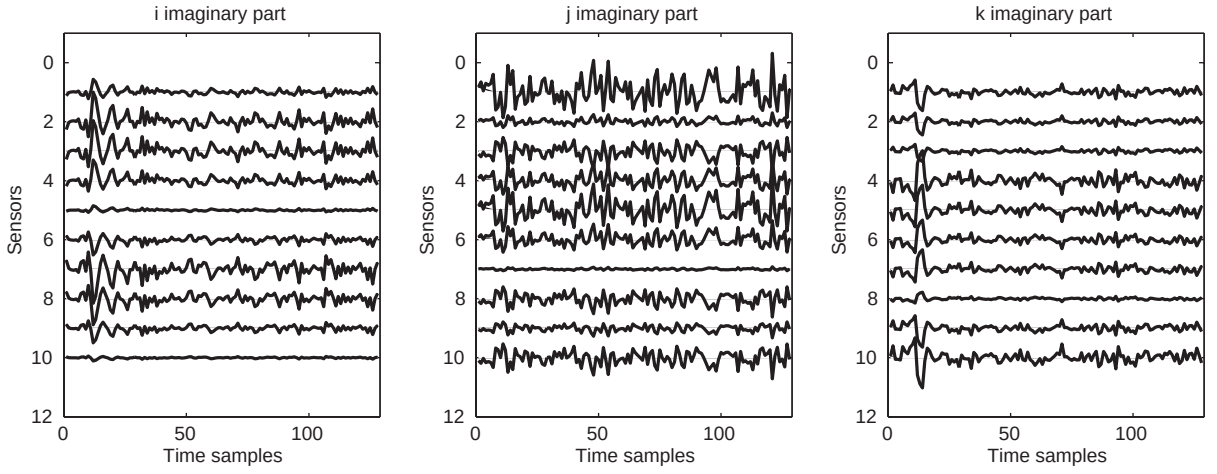

Fig. 12. Mixture 1: signal subspace using classical SVD component-wise.

The sets of singular values obtained by the three component-wise SVDs (Fig. 14) have the same behaviour, showing a high amplitude singular value and the others with lower magnitude. This leads to the construction of the *signal subspace* using three rank-1 truncations of SVDs. The corresponding signal subspace is then presented in Fig. 16.

In the SVDQ case (Fig. 15), the set of singular values has globally the same behaviour as in the component-wise SVD case, except that the ratio between the first and the second singular values is greater using SVDQ (Fig. 15) than in the SVD case (Fig. 14). The signal subspace is also obtained by rank-1 truncation of the SVDQ (Fig. 17).

In *signal subspaces* obtained via SVDQ and SVD techniques, the first wave seems to be well estimated. However, the result is better in the SVDQ case. This can be seen in the noise subspaces presented in Fig. 18 for the SVD component-wise and in Fig. 19 for the SVDQ.

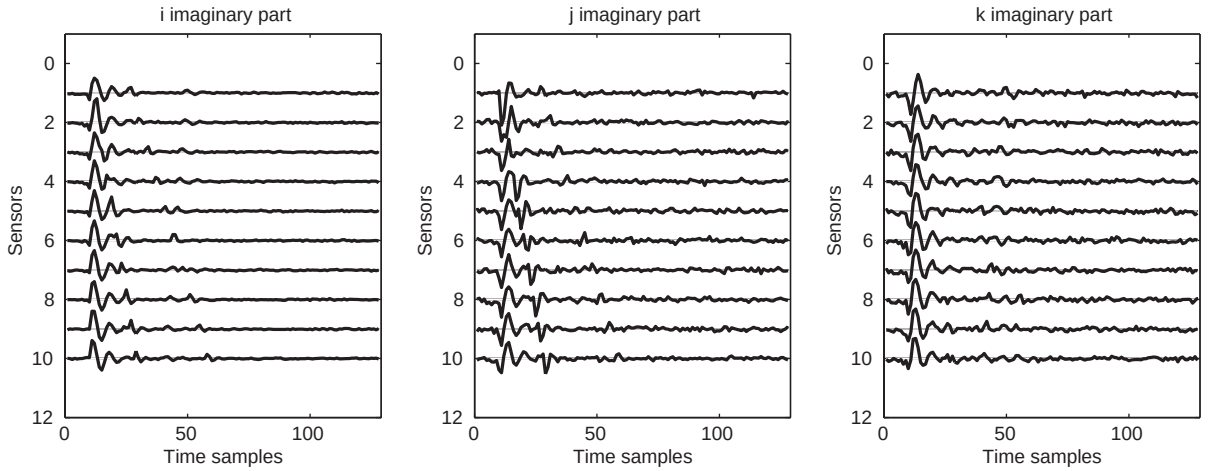

Fig. 13. Mixture 2: four waves and noise.

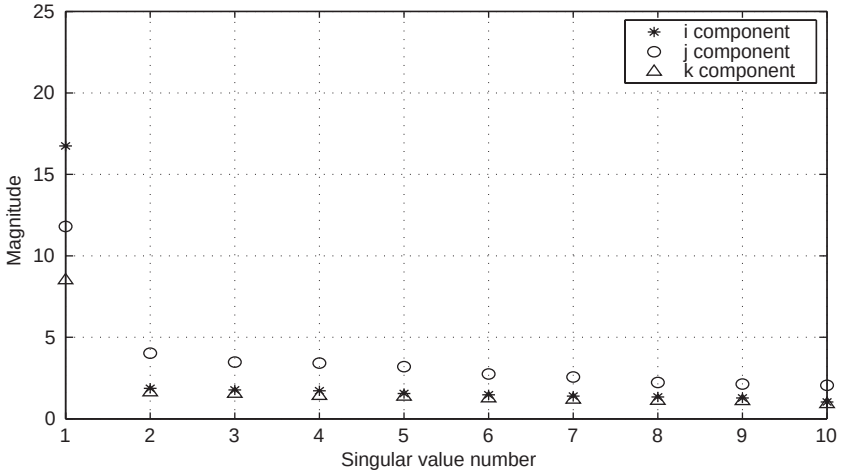

Fig. 14. Mixture 2: singular values obtained by SVD independently on the three components.

In the *noise subspace* obtained by SVDQ (Fig. 19), the first wave is no more visible, due to the good estimation of its three components using the quaternion approach. On the other hand, in the *noise subspace* obtained by component-wise SVD (Fig. 18), some parts of the first wave can be seen (especially on the last sensors of the three components). This is due to a worse estimation of the *infinite velocity* wave in the signal subspaces when processing each component separately. The dispersion of the first wave is the origin of the problem encountered by the component-wise approach. It is known that a dispersive wave needs more than a rank-1 truncation of the SVD to be well estimated [18].

Using SVDQ, the first wave has been well estimated and so waves of lower magnitude can be recovered on the three components (Fig. 19). The polarization and dispersion of the first wave are also estimated correctly in the signal subspace. The quaternion subspace method is not sensitive to phase shifts (dispersion or elliptical polarization) in the way that such physical quantities do not increase the rank of the *signal subspace*. This is not possible using component-wise approach (or subspace method over the real field $\mathbb{R}$).

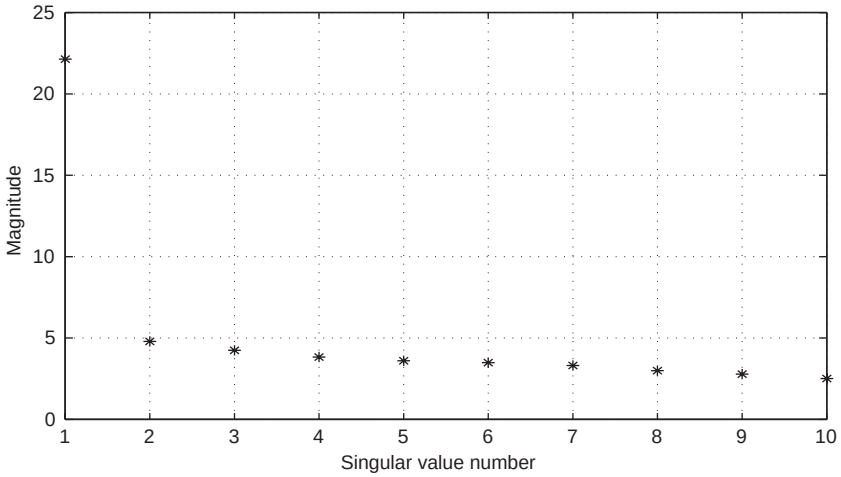

Fig. 15. Mixture 2: singular values obtained by SVDQ.

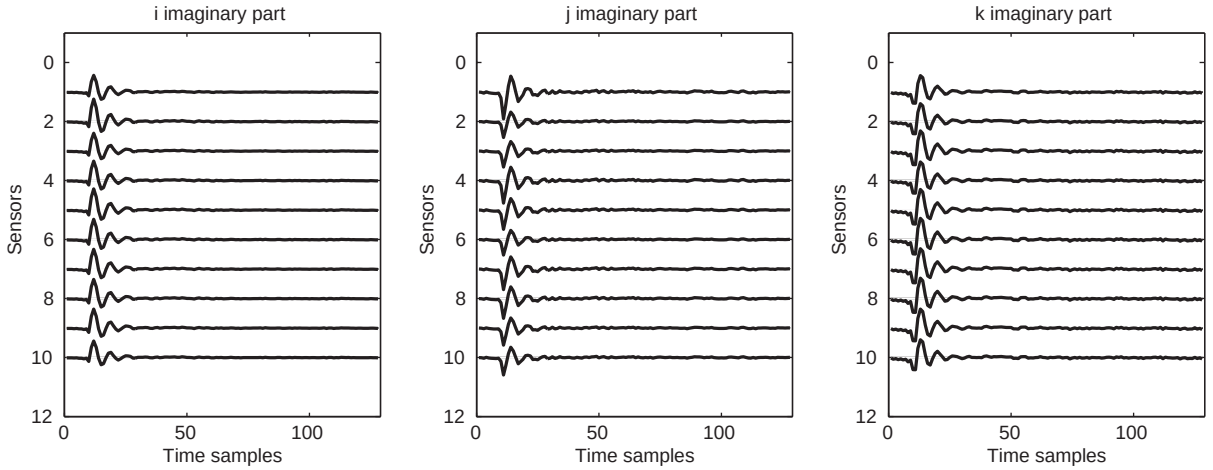

Fig. 16. Mixture 2: signal subspace obtained by classical SVD component-wise.

The sensitivity of *signal subspace* estimation to sensor rotation is very small due to the fact that it corresponds to a rotation in 3D. This can be seen as a phase shift of the quaternionic signal and so it does not affect estimation of the *signal subspace*. So the SVDQ based technique gives the same performance when sensor rotation occurs.

7. Conclusion

We have proposed a new model for vector-sensor array signals based on quaternion algebra. It provides a simple notation for vector signal manipulation and processing. The quaternion approach proposed is valid for sensors having four components (encountered in Geophysics when a pressure sensor is added to a triplet of velocity measurement sensor) and three components. It also includes the case of two components sensors, reducing then to complex case (as $\mathbb{C} \subset \mathbb{H}$).

Quaternion model allows to include wave polarization in algorithms and to take advantage of the signal redundancy on its components. The existence of phase shifts (elliptical polarization or dispersion of waves) between the components does not increase the rank of

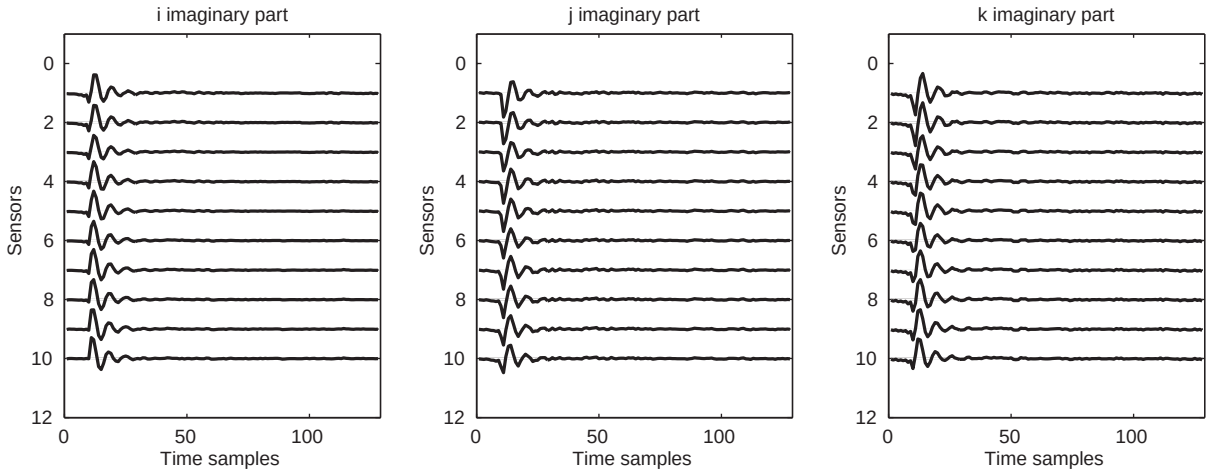

Fig. 17. Mixture 2: signal subspace using SVDQ.

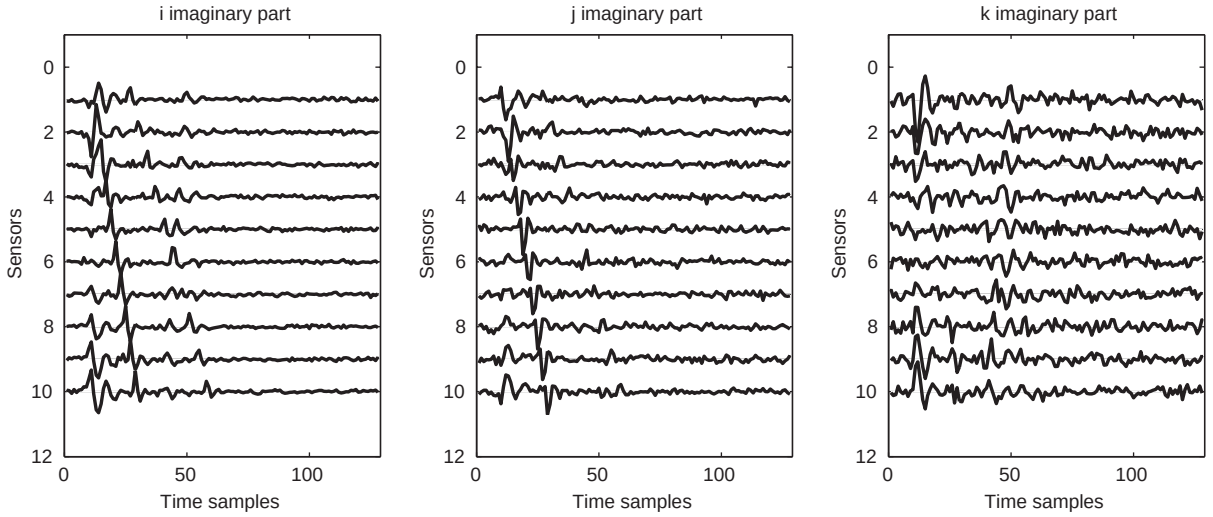

Fig. 18. Mixture 2: noise subspace obtained by classical SVD component-wise.

signal subspace in SVDQ approach, whereas it does in the SVD component-wise approach.

We have proposed a new quaternion subspace method that can be used for polarized wave separation on vector-sensor array. Its superiority upon the component-wise approach (over $\mathbb{R}$) has been shown. The SVDQ technique may also be interesting to recover the component of a polarized signal that is lost in noise. This configuration could be found in communication problem, when one signal is lost in noise in a diversity of polarization transmission technique.

As said above, SVDQ leads to orthogonal bases that fail to separate independent waves and noise. A natural extension of the proposed method would include higher order statistics (ICA-like technique) in order to enhance the separation results and release the constraint of uncorrelation to higher order independence.

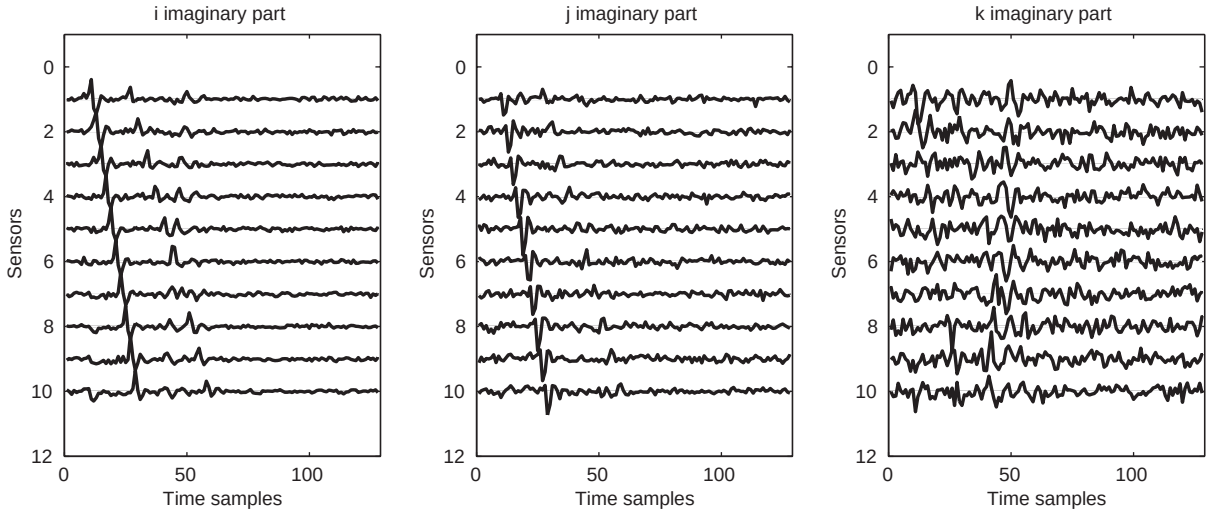

Fig. 19. Mixture 2: noise subspace using SVDQ.

The proposed method is in fact linked with PCA and could be seen as the *standardisation step* in a blind polarized source separation algorithm.

As perspectives to this work, the study of sensors with an arbitrary number l of components could be investigated. The use of hypercomplex number of dimension l to encode could there be used, as well as the use of Clifford Algebras [14,21]. These algebras have already been used to develop pattern recognition algorithm on hyperspectral images [26]. Results obtained herein and in other work using geometric algebra to handle vector signals tend to show that such algebra are a powerful tool for developing algorithm specially dedicated to vector-sensors signal processing.

Appendix A. Phase shift of polarized signals

Using the quaternionic signal representation, any polarized signal is expressed as

$$s_n(m) = \rho_n(m)\mathrm{e}^{\xi_n(m)\pi/2} = \rho_n(m)\mathrm{e}^{\mu_n(m)}. \tag{A.1}$$

This is to say that its magnitude is, at time sample m, equal to $\rho(m)$, and the distribution of magnitude on the three components is carried by the *eigenangle* $\mu(m)$. As $|\mu(m)|_{m=m_0} = 1$, $\forall m_0$, this 3D phase corresponds to a series of point on the 3D unit sphere $\mathscr{S}^2$. So, a constant phase shift, i.e. independent of m, consists in a rotation of all time samples in 3D space. This is to say that a phase shifted version, $s_n^\star(m)$, of a quaternionic signal $s_n(m)$ can be written as

$$s_n^\star(m) = q s_n(m) q^{-1}, \tag{A.2}$$

where $q \in \mathbb{H}$ is a unit quaternion (see [17] for rotations using quaternions). In fact, the rotation operator $q[.]q^{-1}$ only affects the phase of the quaternionic signal, so that we can write

$$s_n^\star(m) = \rho_n^\star(m)\mathrm{e}^{\mu_n^\star(m)} = \rho_n(m)\mathrm{e}^{q\mu_n(m)q^{-1}}. \tag{A.3}$$

Proof. As $s_n^\star(m) = q s_n(m) q^{-1}$, the square of the modulus of $s_n^\star(m)$ is given by

$$\begin{aligned}\rho_n^{\star 2}(m) &= (q s_n(m) q^{-1})(q s_n(m) q^{-1})^* \\ &= q s_n(m) q^{-1} (q^{-1})^* s_n(m)^* q^* \end{aligned} \tag{A.4}$$

$$= \frac{1}{|q|^2}(q s_n(m) q^{-1} q s_n(m)^* q^*) \tag{A.5}$$

$$= \frac{1}{|q|^2} q s_n(m) s_n(m)^* q^* \tag{A.6}$$

$$= \frac{1}{|q|^2}\, q |s_n(m)|^2 q^* = |s_n(m)|^2. \tag{A.7}$$

So

$$\rho_n^{\star}(m) = \rho_n(m) \tag{A.7}$$

which proves that $s_n^{\star}(m)$ and $s_n(m)$ have the same modulus. Then, as any quaternion $q = a + b\mathtt{i} + c\mathtt{j} + d\mathtt{k} = \mathrm{Re}(q) + \mathrm{Vec}(q)$, with $\mathrm{Re}(q) = a$ and $\mathrm{Vec}(q) = b\mathtt{i} + c\mathtt{j} + d\mathtt{k}$, we can write

$$\begin{aligned} s_n^{\star}(m) &= q s_n(m) q^{-1} \\ &= q\mathrm{Re}(s_n(m))q^{-1} + q\mathrm{Vec}(s_n(m))q^{-1} \end{aligned} \tag{A.8}$$

then

$$|\mathrm{Vec}(s_n^{\star}(m))| = \mathrm{Vec}(s_n^{\star}(m))\mathrm{Vec}(s_n^{\star}(m))^{*} \tag{A.9}$$

and so, using the same argument given in (A.4), (A.5) and (A.6), we get

$$|\mathrm{Vec}(s_n^{\star}(m))| = |\mathrm{Vec}(s_n(m))|. \tag{A.10}$$

Then, it is straightforward, using definitions in Eq. (4), that the eigenaxis of $s_n^{\star}(m)$ and $s_n(m)$ are linked as

$$\mu^{\star}(n) = q\mu(n)q^{-1}. \qquad \square \tag{A.11}$$

As polarization information is encoded in the *eigenaxis* of the quaternion signal, it can be useful to visualize the different positions of $\mu(m)$ with time (i.e. for the increasing values of m).

The effect of a phase shift on a polarized signal is a rotation of the polarization curve (Lissajous plot) on the 3D unit sphere.

Appendix B. Subspaces rank and polarized waves

The subspace method presented in Section 5 is a powerful tool for wave separation in the case where the *signal subspace* is a low rank truncation of the data representing the original data set. In the following derivations, we consider that signals and noises collected on vector-sensor arrays are matrices of $\mathbb{H}^{N\times M}$

B.1. Infinite velocity polarized waves are rank-1 quaternion matrices

When considering the SVDQ as a sum of rank-1 matrices, the first so-called rank-1 matrix $\mathbf{S}^{r=1} \in \mathbb{H}^{N\times M}$ is constructed using the first left and the first right singular vectors, and can be expressed as their outer product, multiplied by the corresponding singular value:

$$\mathbf{S}^{(r=1)} = \sigma\mathbf{u}\mathbf{v}^{\triangleleft} = \sigma \begin{bmatrix} u_1 \\ u_2 \\ \vdots \\ u_N \end{bmatrix} [\bar{v}_1 \;\; \bar{v}_2 \;\; \ldots \;\; \bar{v}_M] \tag{B.1}$$

with $u_n, \bar{v}_m \in \mathbb{H}$ and $\sigma \in \mathbb{R}$. Then the first row of $\mathbf{S}^{(r=1)}$ is the row vector $\mathbf{s}_1^{(r=1)} = \sigma[u_1\bar{v}_1 \;\; u_1\bar{v}_2 \;\; \ldots \;\; u_1\bar{v}_M] = [\sigma s_1 \;\; \sigma s_2 \;\; \ldots \;\; \sigma s_M]$. The expression of other rows follows immediately.

Now considering the case where the recorded polarized wave has *infinite* velocity (and is not dispersive), the signals recorded from the second to the Nth sensors are just copies of the signal recorded on the first sensor $\mathbf{s}^{\mathrm{T}}$, up to a (real) scalar amplitude term. This is to say that for infinite velocity waves, the quaternion matrix, say $\mathbf{S}^{\mathrm{inf}}$, that represents its behaviour on the array has the form:

$$\begin{aligned} \mathbf{S}^{\mathrm{inf}} &= \begin{bmatrix} s_1 & s_2 & \ldots & s_M \\ \alpha_1 s_1 & \alpha_1 s_2 & \ldots & \alpha_1 s_M \\ \alpha_2 s_1 & \alpha_2 s_2 & \ldots & \alpha_2 s_M \\ \vdots & & & \vdots \\ \alpha_{N-1} s_1 & \alpha_{N-1} s_2 & \ldots & \alpha_{N-1} s_M \end{bmatrix} = \begin{bmatrix} \mathbf{s}^{\mathrm{T}} \\ \alpha_1 \mathbf{s}^{\mathrm{T}} \\ \alpha_2 \mathbf{s}^{\mathrm{T}} \\ \vdots \\ \alpha_{N-1} \mathbf{s}^{\mathrm{T}} \end{bmatrix}, \end{aligned} \tag{B.2}$$

where $\alpha_i \in \mathbb{R}$ and $s_i \in \mathbb{H}$. The rank of $\mathbf{S}^{\mathrm{inf}}$ is 1 as it can be written as

$$\begin{aligned} \mathbf{S}^{\mathrm{inf}} &= \sigma' \begin{bmatrix} u_1' \\ u_2' \\ \vdots \\ u_N' \end{bmatrix} [\bar{v}_1 \;\; \bar{v}_2 \;\; \ldots \;\; \bar{v}_M] \\ &= \sigma' \begin{bmatrix} \dfrac{1}{\sigma'} u_1 \\ \dfrac{\alpha_1}{\sigma'} u_1 \\ \vdots \\ \dfrac{\alpha_{(N-1)}}{\sigma'} u_1 \end{bmatrix} [\bar{v}_1 \;\; \bar{v}_2 \;\; \ldots \;\; \bar{v}_M], \end{aligned} \tag{B.3}$$

where σ' is such that vector $\mathbf{u}$ is normalized, and $u_1\mathbf{v}^{\triangleleft}=\mathbf{s}^{\mathrm{T}}$. Consequently, when only an *infinite* velocity is in the data set, it is a rank-1 matrix.

B.2. Infinite velocity polarized and dispersive waves are rank-1 quaternion matrices

As explained in Section 4.1.4 and Appendix A, a dispersive wave recorded on a vector-sensor array can be written as

$$\mathbf{S}^{\mathrm{inf/disp}}=\begin{bmatrix}\mathbf{s}^{\mathrm{T}}\\ \alpha_1 q\mathbf{s}^{\mathrm{T}}q^{-1}\\ \alpha_2 q^2\mathbf{s}^{\mathrm{T}}q^{-2}\\ \vdots\\ \alpha_{N-1}q^{N-1}\mathbf{s}^{\mathrm{T}}q^{-(N-1)}\end{bmatrix}, \tag{B.4}$$

where $q\in\mathbb{H}$ and $|q|=1$. This matrix can also be written as the product of two quaternion vectors weighted by a real constant:

$$\mathbf{S}^{\mathrm{inf/disp}}=\sigma''\begin{bmatrix}u_1''\\ u_2''\\ \vdots\\ u_N''\end{bmatrix}[\bar{v}_1''\ \ \bar{v}_2''\ \ \dots\ \ \bar{v}_M'']$$

$$=\sigma''\begin{bmatrix}\frac{1}{\sigma''}u_1\\ \frac{\alpha_1}{\sigma''}qu_1\\ \vdots\\ \frac{\alpha_{(N-1)}}{\sigma''}q^{(N-1)}u_1\end{bmatrix}$$

$$\times[\bar{v}_1\ \ \bar{v}_2 q\ \ \dots\ \ \bar{v}_M q^{-(N-1)}]. \tag{B.5}$$

This demonstrates that a dispersive wave is a rank-1 quaternionic matrix.

B.3. Non-infinite velocity polarized waves are full rank quaternion matrices

When no pre-processing step has been performed on the data set, a recorded polarized wave impinges the set of sensors with different arrival times. Thus, each sensor records a delayed version of the signal recorded on the first one (one of the three components of such a signal is presented in Fig. 5). As we consider instantaneous mixture, a delayed version of a wave is another wave, so that the array of N sensors will see N waves. Denoting the different waves as $\mathbf{s}_1^{\mathrm{T}},\dots,\mathbf{s}_N^{\mathrm{T}}$, the data matrix $\mathbf{S}^{\text{non-inf}}$ is

$$\mathbf{S}^{\text{non-inf}}=\begin{bmatrix}\mathbf{s}_1^{\mathrm{T}}\\ \mathbf{s}_2^{\mathrm{T}}\\ \mathbf{s}_3^{\mathrm{T}}\\ \vdots\\ \mathbf{s}_N^{\mathrm{T}}\end{bmatrix}. \tag{B.6}$$

There is no reason for the lines of $\mathbf{S}^{\text{non-inf}}$ to be correlated, and so any of the quaternionic signals $\mathbf{s}_i^{\mathrm{T}}$ with $i=2,\dots,N$ cannot be written as $\mathbf{s}_1^{\mathrm{T}}$ multiplied by a (real) scalar. Then, each of the N signals $\mathbf{s}_1^{\mathrm{T}},\mathbf{s}_2^{\mathrm{T}},\dots,\mathbf{s}_N^{\mathrm{T}}$ is represented by a rank-1 matrix (see Sections B.1 and B.2). As a consequence, a non-infinite velocity polarized (possibly dispersive) wave is represented by a sum of N rank-1 quaternionic matrices:

$$\mathbf{S}^{\text{non-inf}}=\sum_{i=1}^{N}\mathbf{u}_i\mathbf{v}_i^{\triangleleft}\sigma_i \tag{B.7}$$

This makes $\mathbf{S}^{\text{non-inf}}$ a rank-N matrix.

B.4. Non-polarized noise is full rank quaternion matrix

Consider that each of the N vector-sensors of the array has recorded a white Gaussian noise. Noise recorded on one vector-sensor is independent of noises recorded on other vector-sensors. This is to say that

$$\langle b_\alpha(m),b_\beta(m)\rangle=\gamma^2\delta_{\alpha\beta}, \tag{B.8}$$

where β and α are the sensor position in the array, and the scalar product $\langle .,.\rangle$ is defined in Eq. (11). $\delta_{\alpha\beta}$ is the Kronecker symbol defined and used in Section 5.1. Thus, the set of N Gaussian noises recorded on the N vector-sensors form an orthogonal basis (which is also an independent basis). Consequently, the rank of the quaternion matrix that represents the noise, say $\mathbf{B}\in\mathbb{H}^{N\times M}$, is a full rank matrix ($\mathrm{rank}(\mathbf{B})=\min(N,M)$).

References

[1] S. Anderson, A. Nehorai, Analysis of a polarized seismic wave model, IEEE Trans. Signal Process. 44 (2) (1996) 379–386.

[2] M.R. Andrews, P.P. Mitra, R. deCarvalho, Tripling the capacity of wireless communications using electromagnetic polarization, Nature 409 (6818) (2001) 316–318.

[3] J.L. Brenner, Matrices of quaternions, Pacific J. Math. 1 (1951) 329–335.

[4] L. Brillouin, Wave Propagation and Group Velocity, Academic Press, New York, 1960.

[5] T. Bülow, Hypercomplex spectral signal representations for the processing and analysis of images, Ph.D. Thesis, Christian Albrechts Universität, 1999.

[6] A. Bunse-Gerstner, R. Byers, V. Mehrmann, A quaternion QR algorithm, Numer. Math. 55 (1989) 83–95.

[7] P. Comon, Tensors decompositions. State of the art and applications, IMA Conference of Mathematics in Signal Processing, Warwick, UK, December 18–20, 2000.

[8] L. De Lathauwer, B. De Moor, J. Vandewalle, A singular value decomposition for higher-order tensors, Proceedings of the ProRISC IEEE Workshop on Circuits, Systems and Signal Processing, Houthalen, Belgium, March 24–25, 1993, pp. 37–43, 1993.

[9] E.F. Deprettere, SVD and Signal Processing. Algorithms, Applications and Architecture, North-Holland, Amsterdam, 1988.

[10] T.A. Ell, Hypercomplex spectral transformation, Ph.D. Thesis, University of Minnesota, 1992.

[11] G.H. Golub, C.F. Van Loan, Matrix Computation, Johns Hopkins, Baltimore, MD, 1989.

[12] W.R. Hamilton, On quaternions, Proceeding of the Royal Irish Academy, November 11, 1844.

[13] W.R. Hamilton, Researches respecting quaternions, Trans. Roy. Irish Acad. XXI (1848) 199–296.

[14] D. Hestenes, G. Sobzcyk, Clifford Algebra to Geometric Calculus: A Unified Language for Physics and Mathematics, D. Reidel Publishing Company, Dordrecht, 1984.

[15] L. Huang, W. So, On left eigenvalues of a quaternionic matrix, Linear Algebra Appl. 37 (2001) 105–116.

[16] W.C. Jakes, Microwave Mobile Communications, Wiley, New York, 1974 (reprinted by IEEE press, 1998).

[17] I.L. Kantor, A.S. Solodovnikov, Hypercomplex Numbers, An Elementary Introduction to Algebras, Springer, Berlin, 1989.

[18] N. Le Bihan, Traitement algébrique des signaux vectoriels. Application à la séparation d'ondes sismiques, Ph.D. Thesis, INPG, 2001.

[19] N. Le Bihan, G. Ginolhac, Subspace methods for 3D arrays, Workshop on Physics in Signal and Image Processing (PSIP), 2001, pp. 359–364.

[20] H.C. Lee, Eigenvalues and canonical forms of matrices with quaternions coefficients, Proc. Roy. Irish Acad. Sect. A 52 (1949) 253–260.

[21] P. Lonestou, Clifford Algebra and Spinors, Cambridge University Press, Cambridge, 1997.

[22] M.L. Mehta, Random Matrices, 2nd Edition, Academic Press, New York, 1991.

[23] M. Moonen, B. De Moor, SVD and Signal Processing III. Algorithms, Applications and Architecture, Elsevier, Amsterdam, 1995.

[24] A. Nehorai, E. Paldi, Vector-sensor array processing for electromagnetic source localization, IEEE Trans. Signal Process. 42 (2) (1994) 376–398.

[25] A. Nehorai, E. Paldi, Acoustic vector-sensor array processing, IEEE Trans. Signal Process. 42 (9) (1994) 2481–2491.

[26] E. Rundblad-Labunets, V. Labunets, Spatial-color Clifford algebras for invariant image recognition, in: G. Sommer (Ed.), Geometric Computing with Clifford Algebra. Theoretical Foundations and Applications in Computer Vision and Robotics, Springer, Berlin, 2001.

[27] S.J. Sangwine, Fourier transforms of colour images using quaternion, or hypercomplex, numbers, Electron. Lett. 32 (21) (1996) 1979–1980.

[28] S.J. Sangwine, T.A. Ell, Hypercomplex auto- and cross-correlation of color images, IEEE International Conference on Image Processing (ICIP), Kobe, Japan, 1999, pp. 319–322.

[29] L.L. Scharf, Statistical signal processing, detection, estimation and time series analysis, Electrical and Computer Engineering: Digital Signal Processing, Addison Wesley, Reading, MA, 1991.

[30] L.L. Scharf, The SVD and reduced rank signal processing, Signal Processing 25 (1991) 113–133.

[31] H.D. Schütte, J. Wenzel, Hypercomplex numbers in digital signal processing, IEEE International Symposium on Circuits and Systems, 1990, pp. 1557–1560.

[32] W. So, R.C. Thompson, F. Zhang, The numerical range of normal matrices with quaternions entries, Linear Multilinear Algebra 37 (1994) 174–195.

[33] W.M. Telford, L.P. Geldart, R.E. Sheriff, Applied Geophysics, Cambridge University Press, Cambridge, 1991.

[34] R. Vaccaro, SVD and Signal Processing II. Algorithms, Applications and Architecture, Elsevier, Amsterdam, 1991.

[35] L.A. Wolf, Similarity of matrices in which elements are real quaternions, Bull. Amer. Math. Soc. 42 (1936) 737–743.

[36] V. Zarzoso, A.K. Nandi, Unified formulation of closed-form estimators for blind source separation in complex instantaneous linear mixture, in: M. Gabbouj, P. Kuosmanen (Eds.), Signal Processing X, Theories and Applications, Proceedings of EUSIPCO, Tampere, Finland, 2000.

[37] F. Zhang, Quaternions and matrices of quaternions, Linear Algebra Appl. 21 (1997) 21–57.